

NRL CODE 1200

*Plan level above addressed and
combine with 1000 d.s., 1000/1200
to be in you,
12004*

NRL Report 8677

UNCLASSIFIED

Low-Frequency Acoustic Source Levels of Large Merchant Ships

EVAN B. WRIGHT AND JOHN CYBULSKI

*Large Aperture Acoustic Branch
Acoustics Division*

March 14, 1983



NAVAL RESEARCH LABORATORY
Washington, D.C.

Approved for public release; distribution unlimited.

REPORT DOCUMENTATION PAGE		READ INSTRUCTIONS BEFORE COMPLETING FORM
1. REPORT NUMBER NRL Report 8677	2. GOVT ACCESSION NO.	3. RECIPIENT'S CATALOG NUMBER
4. TITLE (and Subtitle) LOW-FREQUENCY ACOUSTIC SOURCE LEVELS OF LARGE MERCHANT SHIPS	5. TYPE OF REPORT & PERIOD COVERED Interim report on a continuing problem.	
	6. PERFORMING ORG. REPORT NUMBER	
7. AUTHOR(s) Evan B. Wright and John Cybulski (deceased)	8. CONTRACT OR GRANT NUMBER(s)	
9. PERFORMING ORGANIZATION NAME AND ADDRESS Naval Research Laboratory Washington, DC 20375	10. PROGRAM ELEMENT, PROJECT, TASK AREA & WORK UNIT NUMBERS 62759N XF59552100	
11. CONTROLLING OFFICE NAME AND ADDRESS Naval Electronic Systems Command Washington, DC 20360	12. REPORT DATE March 14, 1983	
	13. NUMBER OF PAGES 55	
14. MONITORING AGENCY NAME & ADDRESS (if different from Controlling Office)	15. SECURITY CLASS. (of this report) UNCLASSIFIED	
	15a. DECLASSIFICATION/DOWNGRADING SCHEDULE	
16. DISTRIBUTION STATEMENT (of this Report) Approved for public release; distribution unlimited.		
17. DISTRIBUTION STATEMENT (of the abstract entered in Block 20, if different from Report)		
18. SUPPLEMENTARY NOTES		
19. KEY WORDS (Continue on reverse side if necessary and identify by block number) Shipping noise Radiated noise—merchant ships Supertanker source levels—measurement		
20. ABSTRACT (Continue on reverse side if necessary and identify by block number) Acoustic source-level spectra have been measured for 14 merchant ships, including eight large oil tankers, for the frequency range 2 to 128 Hz. Results are compared with semiempirical cavitation models: a discrete-line model (Gray and Greeley, "Source Level Model for Propeller Blade Rate for the World's Merchant Fleet," Technical Memorandum 458) (Bolt, Beranek, and Newman, Inc., Cambridge, MA), and a model for broadband levels (Ross, "Mechanics of Underwater Noise," Pergamon Press (1976)). The distribution of measured monopole source levels for the second blade harmonics of these ships peaks at about 175 dB re 1 μ Pa, consistent with the Gray-Greeley model, (Continued)		

20. ABSTRACT (Continued)

and individual levels agree within the 6 to 8 dB variance implied by the model. Measured levels in the continuum, at 50 and 100 Hz, average 167 and 161 dB re 1 μ Pa, respectively, about 6 dB below the levels predicted by the Ross model. Below 15 Hz, measured line and broadband levels increase at about 8 dB per octave of decreasing frequency, a systematic difference from cavitation model predictions. This is possibly caused by hull reradiation effects, suggesting a low-frequency limit for the validity of a point-source model for these large ships. This report includes a set of broadside source-level spectra at several ranges for each ship, and tables of ship characteristics and engineering data. These acoustic measurements and the associated data comprise a data bank suitable for further study of ship-generated noise.

CONTENTS

INTRODUCTION	1
DATA PROCESSING	1
TRANSMISSION LOSS DETERMINATION	4
LINE STRUCTURE	8
THE CONTINUOUS SPECTRUM	13
CONCLUSIONS AND RECOMMENDATIONS	15
ACKNOWLEDGMENTS	15
REFERENCES	16
APPENDIX A—Operational Conduct of Experiments	17
APPENDIX B—Ship Photographs	19
APPENDIX C—Measured Source-Level Spectra	27
APPENDIX D—Error Analysis	49

LOW-FREQUENCY ACOUSTIC SOURCE LEVELS OF LARGE MERCHANT SHIPS

INTRODUCTION

The importance of shipping noise as a contributor to ambient noise levels in the ocean has long been recognized. In the last two decades, increases in the amount of shipping, and changes in engineering characteristics of the world's merchant fleet have combined to make shipping noise levels higher than ever before. As stated by Ross, "...one must conclude that in the last 25 years ambient noise has probably risen about 10 dB in those areas where shipping noise dominates, furthermore, ship noise must now have become a dominant factor in some areas where it did not previously control [1].

Models of surface-shipping noise must take into account the newer and larger merchant ship types, such as supertankers, since these ships can be expected to be prime contributors to ambient noise levels in areas where they operate. To get reliable data as input to such models, the Naval Research Laboratory conducted two experiments (in 1975 and 1977) to measure source-level spectra of large merchant ships [2]. In both experiments sonobuoys were deployed in the paths of ships found under way in major shipping lanes in deep water. This report consists of an analysis of the data obtained from 14 subject ships—half of them supertankers—and comparison of the data with available models of the ship noise spectra.

We believe that this set of noise measurements is a unique data base for large merchant ships. The measurement geometry was arranged to make the determination of source-receiver range and transmission loss as straightforward and nearly unambiguous as possible. In each case a row of five sonobuoys, at 926 m spacing, was air-dropped across the ship's track. The sonobuoy depth was 305 m. Usually the drop was successful in centering the buoy line across the track, so that there were receivers on each side of the ship with ranges at closest approach (CPA) between about 400 and 1300 m. At these ranges from the source, sound reception uncontaminated by either bottom reflections or Lloyd's mirror interference fringes, for the frequency range 2 to 128 Hz, could be achieved. Appendix A, which is extracted from Ref. 2, describes the conduct of the aircraft operations and sound recording in more detail.

The data base consists of a set of 14 5-channel acoustic recordings, each about 20 min long, and also a fairly complete set of acoustically important engineering parameters for the subject ships. Each ship was identified, and in most cases the operating companies responded to inquiries with information about ship dimensions, propeller characteristics, and operating conditions at the time of observation. Table 1 summarizes the experimental parameters and the operating characteristics for each ship. Appendix B contains photographs of several of the ships at the time of measurement. Table 2 is a summary of the measured source levels for the first three blade frequencies and broadband levels for two selected frequencies in the continuum.

DATA PROCESSING

The acoustic recordings were initially digitized at a frequency resolution of 1 Hz, with 75% overlap; i.e., spectra representing 1 s of integration time were generated at intervals of 1/4 s. A hardware fast Fourier transform with Hanning tapering was used in this initial stage. The digital data base thus

WRIGHT AND CYBULSKI

Table 1 — Characteristics of Subject Ships

Ship	Type*	Power Plant†	Flag	Built	Date	Latitude	Longitude	Water Depth (m)	Estimated Wave Height (ft)
Australian Endeavour	Cont	2 ST	Australia	1969 (W Germ)	1/16/77	32 25N	14 39W	4350	3
Belcarg	Ore	DD	Norway	1975	1/23/77	33 12N	13 13W	4250	3
Blumenthal	Refr	2 DD	W Germ	1974	1/19/77	37 05N	00 10W	2650	3
Chase Venture	Tank	2 ST	Liberia	1975 (Japan)	1/16/77	32 20N	14 29W	4350	3
Esso Kagoshima	Tank	2 ST	Liberia	1973 (Japan)	8/29/75	39 39N	11 18W	4500	3
Flora N	Bulk	DD	Greece	1973 (Taiwan)	1/19/77	37 26N	02 18E	2700	2
Lagena	Tank	ST	W Germ	1974	8/31/75	39 05N	11 24W	4000	2
Lottia	Tank	2 ST	W. Germ.	1975	1/15/77	34 18N	13 34W	4400	3
Manhattan Prince	Tank	DD	Singapore	1974 (Japan)	1/19/77	37 27N	02 17E	2700	2
Mostoles	Tank	DD	Spain	1970	8/27/75	34 26N	09 54W	4300	2
Sea Saint	Tank	2 ST	Sweden	1974	1/22/77	33 58N	14 05W	3950	1
Takara	Bulk	DD	Norway	1968 (Japan)	1/23/77	32 59N	13 33W	4300	3
Thor	Bulk	DD	W. Germ.	1973	1/22/77	31 18N	14 14W	3600	1
World Dignity	Tank	2 ST	Liberia	1975 (Japan)	8/29/75	36 04N	12 34W	5000	3

- * Cont : High-Speed Container Ship
- Ore : Ore Cargo Ship
- Refr : Refrigerated Cargo Ship
- Tank : Oil Tanker
- Bulk : Bulk Cargo Ship

- † ST : Steam Turbine
- DD : Direct-Drive Diesel

Table 1 — Characteristics of Subject Ships (Continued)

Ship	Course	Speed (kt)	rpm	Tonnage (1000 DWT)	Length (m)	Beam (m)	Draft (m)	Shaft Depth (m)	Propeller Diameter (m)	Blades
Australian Endeavour	199	20.0	122	14	217	29	10.0	6.2	6.3	4
Belcarg	044	15.0	111	109	266	38	13.9	9.9	6.8	4
Blumenthal	259	19.7	128	12	146	22	9.5	4.5	6.0	4
Chase Venture	199	11.9	61	280	340	53	21.6	4.1	8.6	5
Esso Kagoshima	022	14.5	83	257	338	52	20.3	14.4	9.2	5
Flora N	251	13.6	117	29	181	25	10.4	4.6	6.0	4
Lagena	019	14.6	78	312	351	56	22.1	15.2	9.2	4
Lottia	177	15.5	72	317	321	56	12.3	5.8	9.2	4
Manhattan Prince	085	16.2	107	85	245	38	13.7	8.0	6.0	5
Mostoles	042	12.6	114	103	266	39	19.6	14.6	6.3	4
Sea Saint	197	13.2	66	356	362	60	13.1	7.1	9.1	5
Takara	015	13.1	104	57	224	32	11.6	7.6	5.9	5
Thor	190	15.5	100	146	303	43	12.2	7.9	7.4	7
World Dignity	022	17.7	86	271	337	54	21.0	13.0	8.6	5

Table 2 — Summary of Experimental Results

Ship	Estimated Cavitation Depth (m)	Measured CPA Ranges (m)		Measured Line Frequencies (Hz)		Monopole Blade Line Levels (dB re μ Pa @ 1m)				Monopole Broadband Levels (dB re μ Pa/Hz @ 1m)			
		R	L	Shaft	Blade	Measured			Model Predictions	Measured		Model Predictions	
						f_1	f_2	f_3	f_1, f_2, f_3	50 Hz	100 Hz	50 Hz	100 Hz
Australian Endeavour	4.0	473	473	2.0	8.0	197	185	182	175	172	159	173	169
Belcarga	7.6	472	262	1.9	7.5	189	174	168	176	164	156	173	169
Blumenthal	2.4	400	599	2.1	8.5	185	173	165	175	163	157	174	169
Chase Venture	1.1	470	—	1.0	5.1	197	189	177	175	172	164	165	160
Esso Kagoshima	11.1	400	553	1.4	6.9	196	181	179	182	169	164	174	170
Flora N	2.5	390	543	1.9	7.7	185	186	181	173	170	162	171	167
Lagena	12.0	430	518	1.3	5.2	200	182	174	177	166	161	172	167
Lottia	2.6	408	445	1.2	4.8	197	188	180	176	166	153	170	165
Manhattan Prince	5.9	179	700	1.8	8.9	190	180	176	176	166	166	170	165
Mostoles	12.4	444	444	1.9	7.5	193	175	174	174	166	165	172	167
Sea Saint	3.9	950	929	1.1	5.5	192	183	180	178	177	160	168	164
Takara	5.5	170	635	1.7	8.6	184	174	170	175	165	160	169	164
Thor	5.3	272	620	1.7	11.6	187	173	169	186	161	161	175	171
World Dignity	10.0	405	492	1.4	7.2	193	183	178	181	163	161	174	169

created was used as the input to second-stage Fourier analyses (zoom FFTs) at finer frequency resolutions. Most of the zoom-FFTs, such as those used for the source-level spectra of Appendix C, were done at a frequency resolution of 1/4 Hz, in the frequency band 0 to 128 Hz. The finest resolution used, in analyzing blade-line widths, was 1/64 Hz. In all cases, a software FFT with Hanning tapering was used in the zoom processing.

Figure 1 shows typical spectra, in which discrete lines are seen well above the continuum at frequencies up to 100 Hz. The logarithmic plot versus frequency accentuates the periodic nature of the discrete line structure. These spectra satisfy one essential condition for making reliable source-level measurements at all frequencies: the levels rise above background, over the whole band, during time of ship passage. This condition was satisfied for all 14 ships analyzed. The highest curve is a beam-aspect spectrum (at CPA); the *stern* and *end* spectra are at angles of 82° and 87° beyond beam. The 15-dB rise in level as the ship passes was typical for all ships. The lowest curve is a system noise spectrum in the absence of signal, calibrated as a *received level* for comparison.

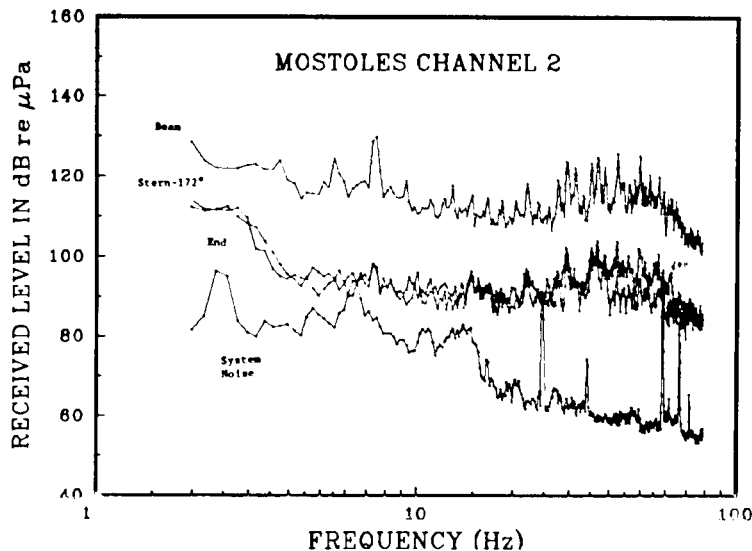


Fig 1 — Received-level spectra for a large diesel tanker

UNCLASSIFIED

The rise in received level is used to estimate the time of the closest approach of the ship (CPA), and to determine between which two buoys the ship passed. In Fig. 2, received level versus time for a spectral line (blade-rate line) and for a 1-Hz region of the broadband spectrum are shown. Evidently, the time of CPA can be determined to within 10 s.

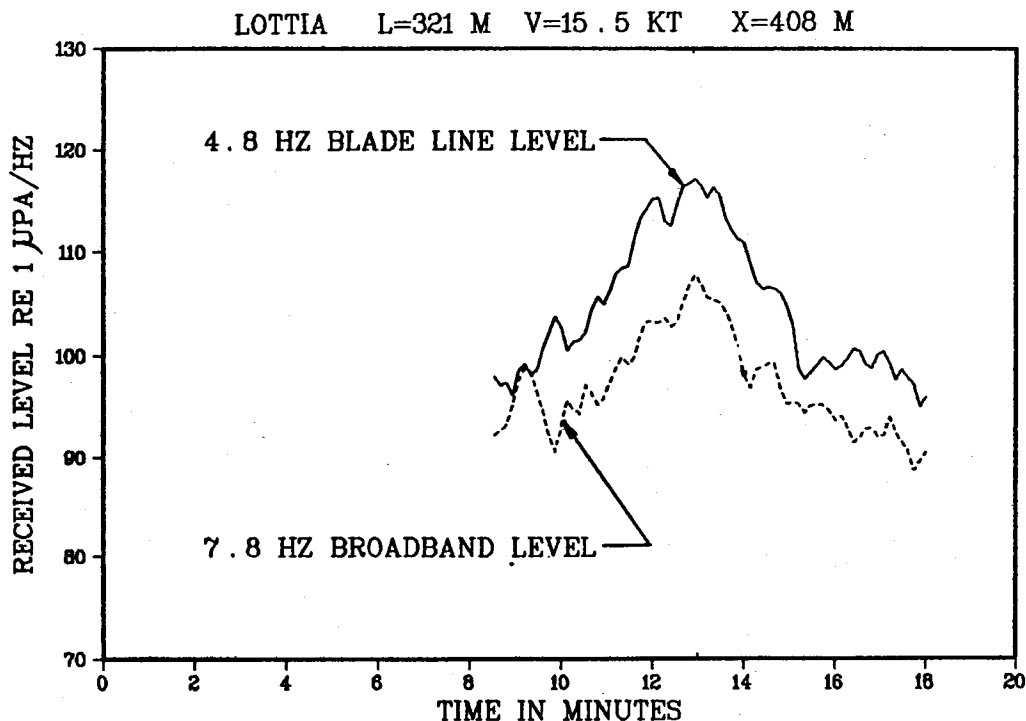


Fig. 2 — Received-level time histories for a large steam-powered tanker, showing the peak at CPA

TRANSMISSION LOSS DETERMINATION

The inertial navigation system of the aircraft was used to track the target ship, and to record the locations of the buoys. Figure 3 shows a typical ship track, with some of the fixes from which the track was estimated. The computed track is a constant-speed rhumb line obtained by a least-squares fit to the fixes. The track estimates generally agreed well with operator reports of course and speed, but they were not accurate enough in relation to the buoy locations to be used for source-receiver ranging. Examination of the acoustic recordings generally showed unambiguously where in the buoy line the ship passed; therefore, we have used the acoustic data for source-receiver ranging, and have based the calculation on the closest receivers to the ship's track; i.e., those for which bottom returns can be neglected. We assume that the source of radiated noise is propeller cavitation, and that this source is localized at a point between the propeller shaft and the top of the propeller disk. This means that all source depths in the measurements were less than about 12 m below the surface, so that surface interference effects are important. Accordingly, the transmission-loss calculation adopted was a simple isovelocity calculation of the direct and surface-reflected path lengths, and coherent addition of the two rays. The ranging and transmission-loss calculation procedure is summarized as follows:

- Determine the two closest buoys and the CPA times (the ship track data is helpful in determining whether CPA occurred simultaneously at all buoys).

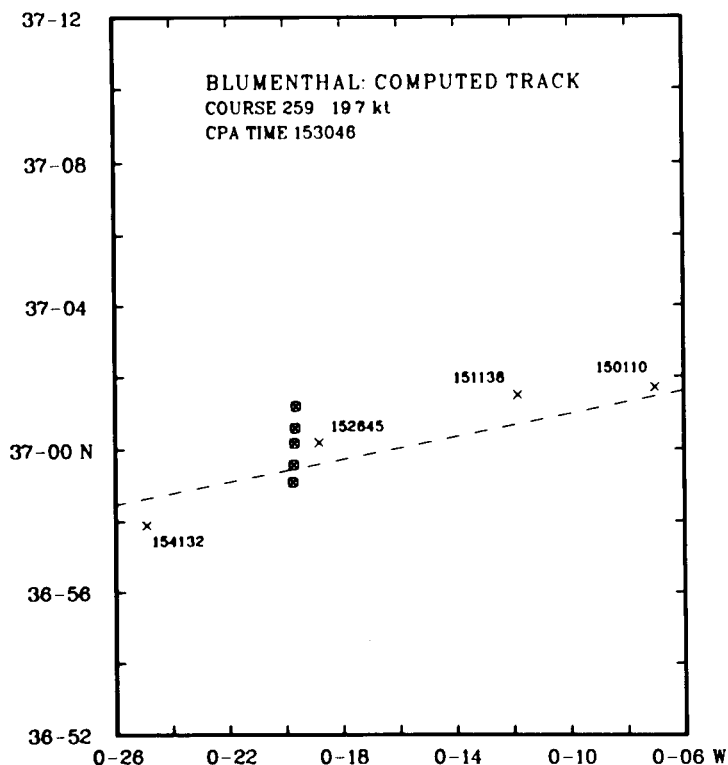


Fig. 3 — A computed ship track with aircraft fix locations and buoy locations from inertial navigation data

- For the two closest receivers, compute the mean received levels for the first three blade lines. Since transmission loss varies approximately as $40 \log r$, where r is the slant range, preliminary estimates of the two CPA ranges can be made.
- Using these estimates, compute mean source levels for the first three blade lines at the two buoys. Correct the range estimates and repeat the source level computation until these mean levels agree. In each step, a *two-minute mean* source level about CPA is computed by calculating transmission loss separately for 30 locations on the track, 4 s apart in the data record.

This procedure assumes that the blade lines are produced by an omnidirectional point source (we have assumed right-left symmetry and no dependence on depression or horizontal aspect angles; the Lloyd mirror dipole pattern is built into the transmission loss calculation). The resultant spectra are for a monopole source at 1 m. One measure of the validity of the assumptions is how well the curves correspond over the whole frequency range, for different buoys. Figures 4 and 5 show some comparisons for buoys within the 200 to 1300 m range window and give an idea of the variability of the results.

In addition to these source level spectra—essentially broadside measurements—we show in Figs. 6 to 9 some polar plots of source level versus horizontal aspect angle for four blade lines of the World Dignity. Cybulski [2] computed these levels from the NRL data by using a wave-theoretic (FFP) program [3] for transmission-loss determination, and comparing the results obtained when the bottom was assumed to be (a) completely reflecting, and (b) completely absorbing. As the angle from broadside increases (along with the range from ship to receiver), a point is reached where the two FFP calculations differ by more than 6 dB; at this point the effect of the bottom is assumed to be unknown and the plot is cut off. For smaller angles the mean of the two transmission-loss calculations is used. In the figures bow aspect is on the positive ordinate axis (top of figure), and corresponding pairs of

WRIGHT AND CYBULSKI

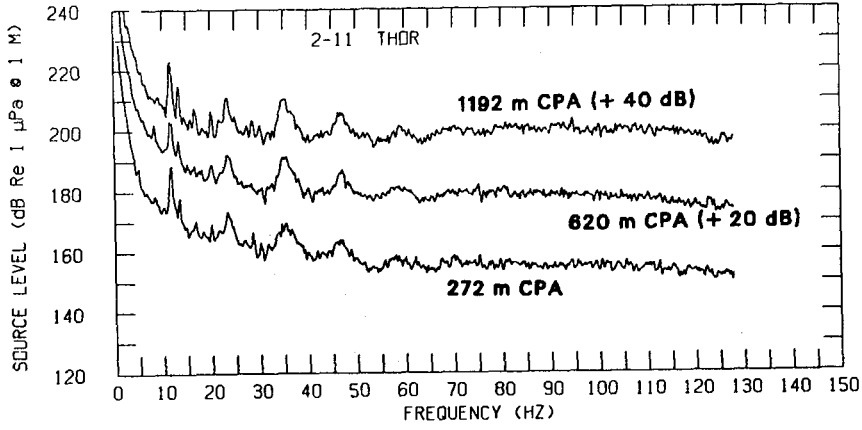


Fig. 4 — Source level spectra for Takara at three CPA ranges

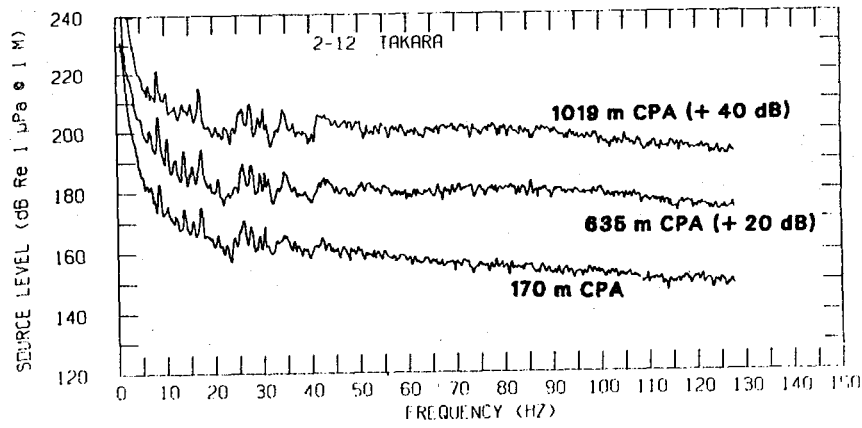


Fig. 5 — Source level spectra for Thor at three CPA ranges

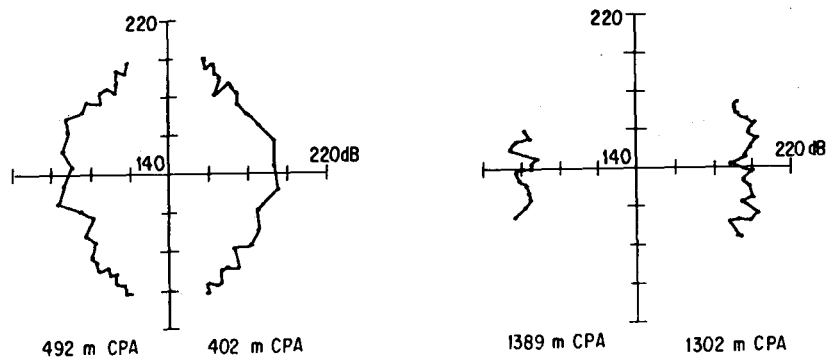


Fig. 6 — Source level directionality for World Dignity blade fundamental (7.2 Hz)

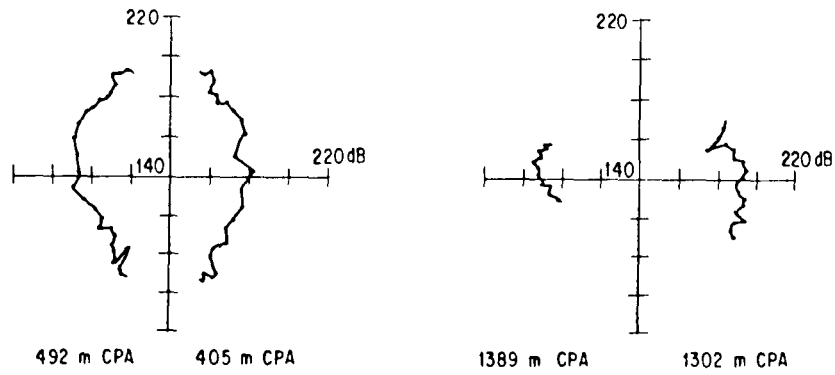


Fig. 7 — Source level directionality for World Dignity first blade harmonics (14.4 Hz)

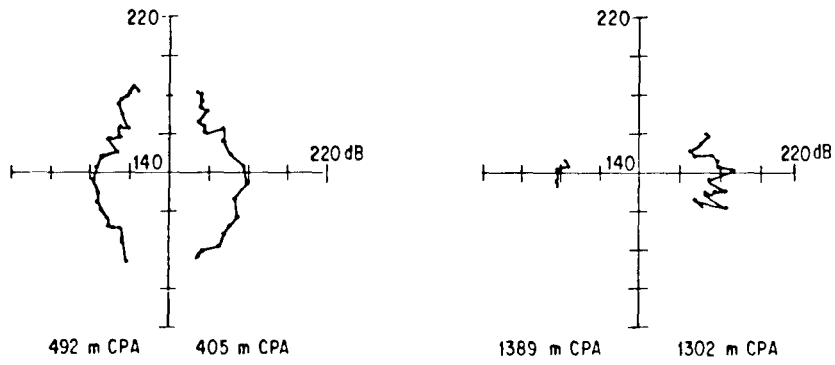


Fig. 8 — Source level directionality for World Dignity second blade harmonics (21.6 Hz)

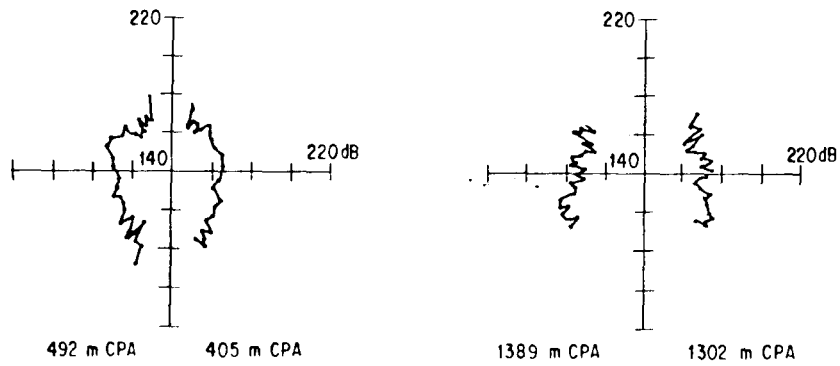


Fig. 9 — Source level directionality for World Dignity fifth blade harmonics (43.2 Hz)

receivers on right and left are plotted together. The plots mostly show increasing levels for aspect angles approaching bow and stern but it should be borne in mind that the computed transmission loss had Lloyd-mirror interference from a perfectly reflecting surface *built in*. This condition may not be satisfied for the higher aspect angles because the ship's hull gets in the way, or because scattering from the ship's wake and at longer ranges (smaller angles of incidence at the surface) reduces the amplitude of the image source. In any case, the plots show no systematic directionality within the 2-min segment of the data that was used for the broadside source level calculation. This segment includes angles up to about $\pm 53^\circ$ from beam aspect for the closest receiver, and up to about $\pm 21^\circ$ for the farthest.

Appendix D is an outline of an error analysis of the procedure. Estimates of errors in the parameters used in the calculation are used in propagation-of-error formulas to estimate the uncertainty in the computed levels. The analysis shows that, of the sources of error considered, uncertainties in hydrophone calibration and source depths are dominant sources of error in the measured levels. Because of the large number of hydrophones used, they were not calibrated individually; instead an average calibration curve was used. The standard deviation of the calibration curve was about 2 dB. The source depth used for each ship was an estimate of the depth of maximum cavitation on the propeller: the shaft depth minus 35% of the propeller diameter. The transmission loss varies as $20 \log y_s$, where y_s is the source depth, so that the computed source level is quite sensitive to errors in this estimate, especially for smaller ships or for tankers not fully ballasted.

LINE STRUCTURE

Appendix C consists of a set of source-level spectra for all 14 ships processed for this report. The spectra are clearly dominated, up to about 60 Hz, by a series of discrete lines. These are harmonics of the propeller shaft frequency n . If B is the number of blades on a ship's propeller, the blade frequency $f_1 = nB$. The blade frequency line and its harmonics are invariably higher in level than the rest of the shaft-rate harmonics. For the diesel ships, a *firing-rate* line, typically $f = 9n$, is comparable in level with the blade lines.

We compare our blade-line results with the semi-empirical model of Gray and Greeley [4]. This is a cavitation model which relates monopole line level, L_b , for the first few blade lines to only two parameters, f_1 , the blade fundamental frequency, and V_m , the maximum cavitation volume on a propeller blade during a revolution:

$$L_b = 20 \log \left| \frac{\pi f_1^2 \rho V_m}{2\sqrt{2} r} \right|,$$

where ρ is the density of the medium and r is the reference range. The maximum cavitation volume is estimated by the empirical relation

$$V_m = 3(10^{-5}) D^3,$$

where the propeller diameter D is in meters.

It is often desirable to characterize merchant shipping as distributed in two fundamental parameters: ship length and speed, empirical formulas to relate blade frequency and propeller diameter to ship length in meters in the Gray-Greeley model are:

$$f_1 = 8 \text{ Hz}, \quad D = 0.12 L^{3/4},$$

where the propeller diameter D and ship length L are in meters. In comparing the NRL measurements with the Gray-Greeley model [4], we can use the actual known propeller parameters. Figures 10, 11, and 12 are plots relating measured and predicted levels for the first three blade lines for all 14 ships. The mean and standard deviation of the difference is shown for each graph. These measured-predicted differences are very large for the blade fundamental, and decrease markedly as the harmonic number

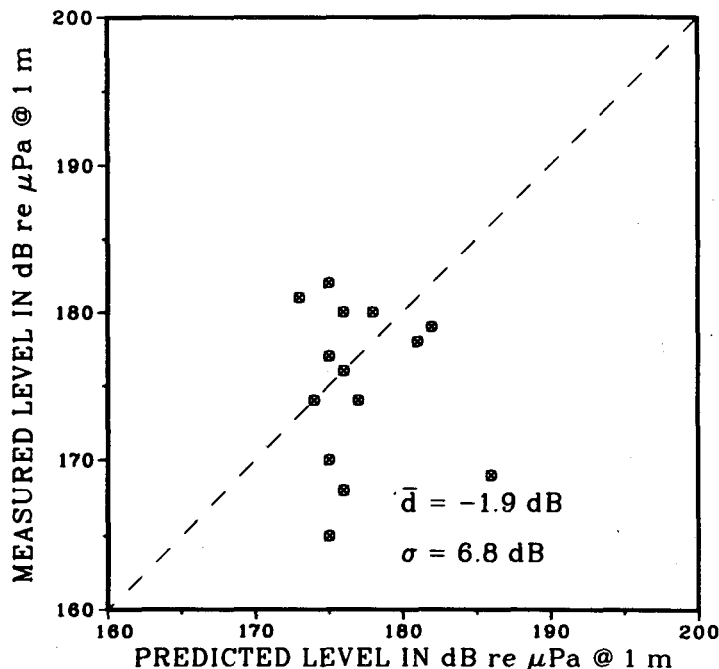


Fig. 12 — Measured source levels vs model predictions for second blade harmonics of 14 ships

increases, while the standard deviation is about 6 dB for each comparison. This standard deviation is about the same as that attributed in Ref. 3 to the empirical formula above, relating maximum cavitation volume to propeller diameter.

The model predicts that the first three blade lines of a given ship will have equal source level. It is evident that our measurements disagree markedly for frequencies below about 15 Hz, or approximately for the first two blade lines. For the third blade line, the differences between measurement and model are within the variances estimated by Gray and Greeley: about 8 dB [4]. The measured levels suggest strongly that the cavitation model is inadequate for large ships, below about 15 Hz.

A useful way of presenting source-level data is in the form of a probability distribution of source levels. Gray and Greeley applied their semiempirical model to an estimated distribution of ship parameters in the world merchant fleet, and produced estimated source-level distributions as functions of ship size class and source depth. The appropriate comparison for the NRL data sample is their estimated distribution for all world merchant ships over 700 ft in length, with source depth taken as 32 ft. Figure 13 shows the distribution of the NRL data (12 ships over 700 ft in length) plotted as solid bars, with the Gray-Greeley distribution plotted as dashed bars. The NRL data set is for the second blade harmonic; i.e., for the frequencies above about 15 Hz. Our sample peaks at about the same level as the model distribution, but has less variance about the peak.

The discrete lines in a ship spectrum are of a complex nature. Figure 14 is a plot of a time-series of received-level spectra in a 1-Hz interval about the blade fundamental of the World Dignity, a large steam-powered tanker. Time increases down the page at 8-s intervals. An arbitrary *floor* simplifies the plot except in the high-intensity time window near CPA. The frequency of the blade harmonic oscillates in sawtooth fashion about its mean value of 7.2 Hz, with a period of about 2 min. The amplitude of this oscillation, about 0.1 Hz, is large enough to obscure the doppler-shift knee on the

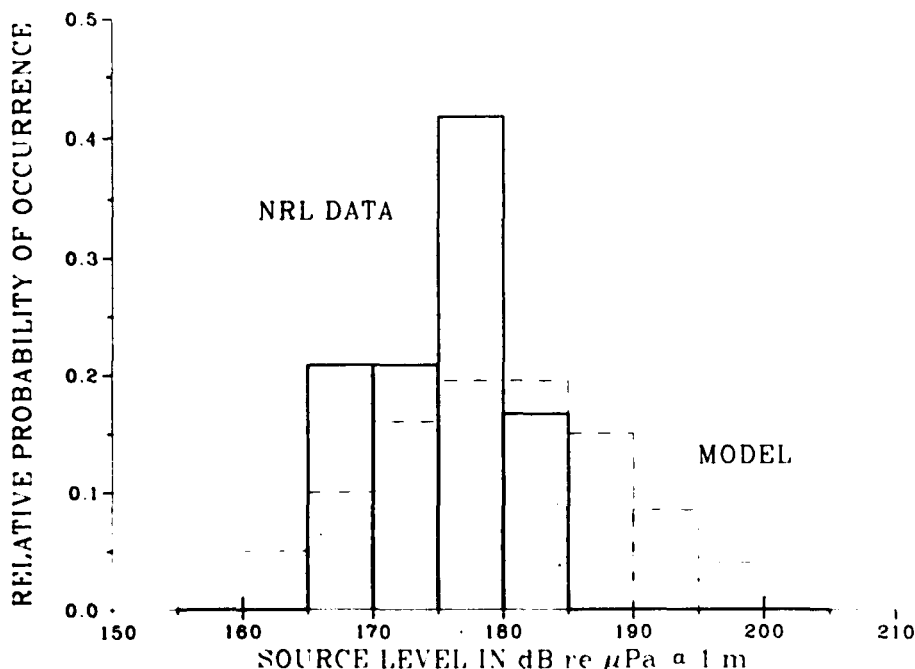


Fig. 13 — Frequency distribution of measured second blade harmonic source levels for 12 large ships, with predicted distribution for world merchant fleet

curve. The other blade lines of this ship show the identical oscillation, with amplitude proportional to line frequency, indicating that the propeller shaft rate varies about $\pm 1.0\%$ about its mean value, presumably because of long-term shaft depth or wake variations for a ship under way. Most ships showed this kind of long-term line frequency variation, with the median amplitude 0.3% of mean line frequency.

In addition to a long-term frequency variation, the discrete lines in the ship spectra have complicated structures, which appear to include sidebands. It is not possible to characterize the spectral lines adequately by simple 3-dB bandwidths; we have selected the weighted root-mean-square bandwidth as the method of computing line width. This is defined, as by Shooter et al., [5] by the equation:

$$BW = \frac{\sum_{i=1}^{N_w} (C_i - N) \cdot (f_i - \bar{f})^2}{\sum_{i=1}^{N_w} (C_i - N)}, \text{ where}$$

f_i is the frequency corresponding to the i th Fourier amplitude C_i of the frequency spectrum, N is a noise floor estimate for the Fourier amplitudes in the summation window from $i = 1$ to N_w , and \bar{f} is a weighted mean frequency:

$$\bar{f} = \frac{\sum_{i=1}^{N_w} (C_i - N) f_i}{\sum_{i=1}^{N_w} (C_i - N)}$$

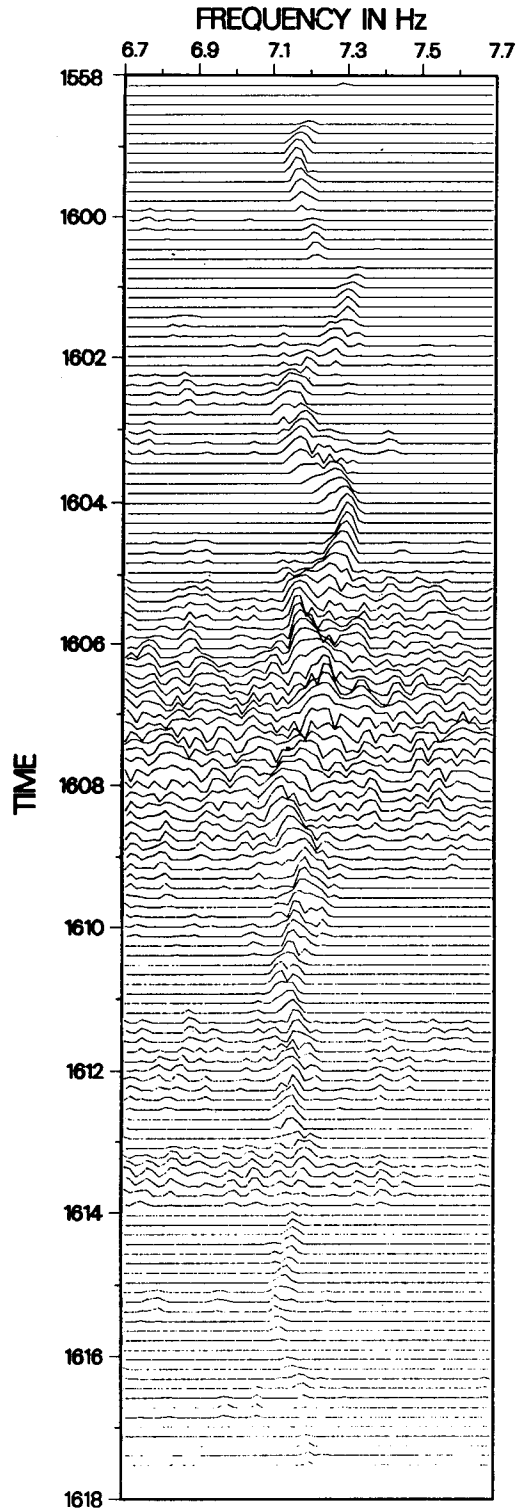


Fig. 14 — Time sequence of received-level spectra in a 1-Hz interval about blade-rate frequency for the World Dignity, a large steam-powered tanker

The computed rms line widths depend, of course, upon the width of the summation window. We have tried to select the summation windows and noise power estimates objectively to enclose the entire line structure, but it is not always possible to choose values unambiguously. We have used a basic maximum summation window width given by:

$$\begin{aligned}
 W &= .75 & f_b < 12, \\
 W &= .75 + .02 \times (f_b - 12) & 12 < f_b < 49.5, \text{ and} \\
 W &= 1.5 & f_b > 49.5,
 \end{aligned}$$

where f_b is the nominal value of the line frequency. For steam-powered ships appearing to have a *pedestal* structure about the blade lines, this was increased by an arbitrary factor of 2.0, but the window was never broadened enough to enclose adjacent shaft lines.

Noise floor estimates are computed by considering a frequency window of width W , centered at the line frequency, and searching the 1.5-Hz interval just below this window for the 0.25-Hz subinterval of lowest power. (This subinterval contains 16 samples at a *binwidth* of 1/64 Hz.) A similar upper noise-floor estimate, for a subinterval just above the summation window, is also computed. The mean of the upper and lower values is used as the noise-floor estimate.

Figure 15 is a composite plot of rms blade-line widths for several ships, plotted as a function of blade-line number. Evidently, the rms widths are roughly proportional to harmonic number, which is predicted by an analysis of cavitation power spectra [6].

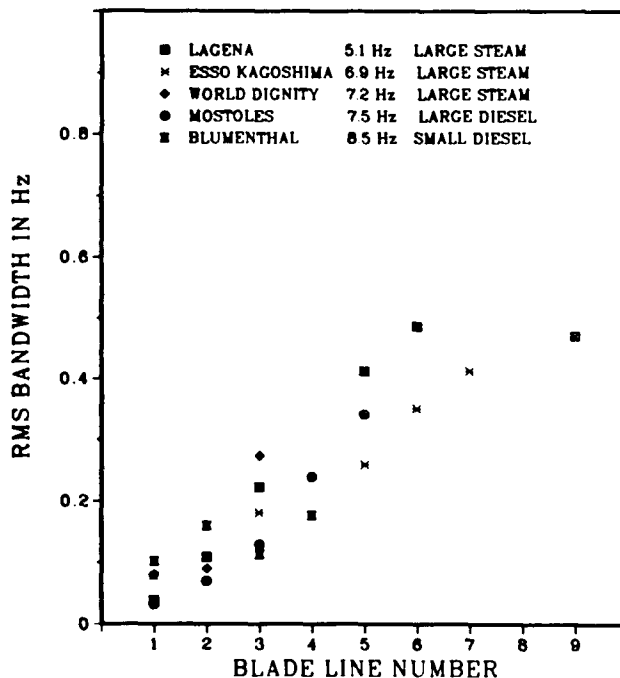


Fig. 15 — Composite rms blade-line bandwidths for five ships

THE CONTINUOUS SPECTRUM

As the measurements indicate, merchant ships produce both discrete lines and a broadband continuum. This continuum is attributed, according to theory, to the same propeller cavitation that produces the blade and shaft lines, and the broadband level should reach a maximum between 50 and 100 Hz.

An analytical model for broadband source level in the continuous spectrum is that of Ross [1], which relates monopole source level, L_{bb} , to propeller tip speed, U_t , and number of blades, B , by the formula

$$L_{bb} = L_0(f) + 60 \log \frac{U_t}{25 \text{ m/s}} + 10 \log \frac{B}{4},$$

where $L_0(f)$ is an empirical function of frequency. In Figs. 16 and 17, measured broadband levels are plotted against levels predicted by the Ross model for two frequencies, 50 and 100 Hz, the mean difference and standard deviations for these curves are comparable with those for the discrete-line comparisons.

Theoretically modeled broadband source levels invariably decrease monotonically on either side of a peak frequency generally between 50 and 100 Hz. The measured source level spectra tend to have peaks in this frequency range, but they also show a sharp rise with frequency decreasing below about 15 Hz. One possible cause which was considered for these large low-frequency values was induced flow noise in the turbulent boundary layer on the ship's hull [7]. To test whether this dipole radiation might have been detected in our short-range measurements, the flow-noise-induced levels were computed as functions of time for extended sources simulating all 14 ship hulls passing the sonobuoys. The computed received-level spectra agree well in frequency dependence with the measured levels, down to about 4 Hz, but they are 10 dB or more lower than the measured levels. Also, the measured shaft- and blade-line levels appear to increase with decreasing frequency in the same fashion. A tentative hypothesis is that the lines excite hull vibrations which reradiate energy detectable at short range, and that the *broadband* energy detected consists of *pedestals* and sidebands of the lines.

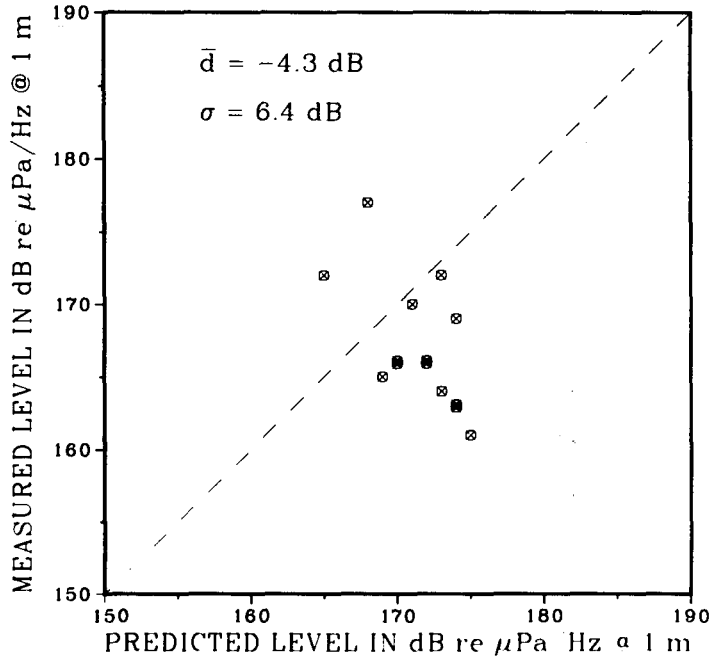


Fig. 16 — Measured source levels vs model predictions for the frequency continuum at 50 Hz, for 14 ships

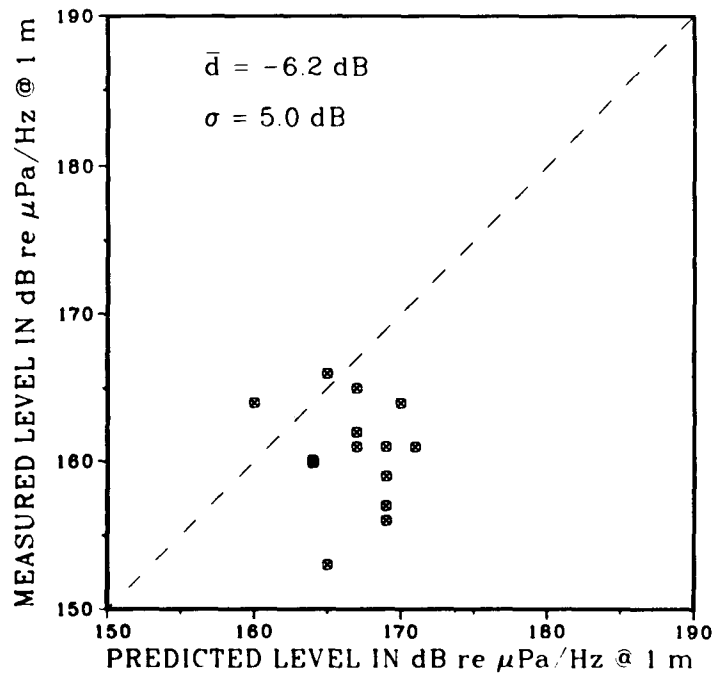


Fig. 17 — Measured source levels vs model predictions for the frequency continuum at 100 Hz for 14 ships

CONCLUSIONS AND RECOMMENDATIONS

In the NRL experiments, air-dropped sonobuoys were used successfully for source-level measurements of 14 ships. With our receiver depth of 305 m, measurements in the frequency range of 15 to 128 Hz can be made with two buoys at about 300 to 600 m and 800 to 1200 m from the ship's track. The method of dropping an equally spaced line of five buoys produced this result in almost all cases. The error analysis indicates that our measured source levels are valid to within ± 6 dB in the frequency range 15 to 128 Hz.

The observed increase in blade-line level with decreasing frequency, below about 15 Hz, is not predicted by a recently formulated shipping noise model [4]. Above this frequency, our measured monopole blade-line levels are comparable with model predictions, within an estimated variance about equal to that predicted by the model. The rising levels at the lowest frequencies may be caused by reradiation from the ship's hull; this question should be investigated further. Root-mean-square blade-line bandwidths are approximately proportional to blade-line number, and this is likewise consistent with current model predictions.

Our measured broadband levels at two selected frequencies are about 6 dB below the monopole levels predicted by the Ross model, with variance also about 6 dB.

It is recommended that further studies be conducted of blade-line width and line structure. The NRL shipping noise data base is a uniquely appropriate and convenient resource for such studies.

ACKNOWLEDGMENTS

Thanks to Dr. Orest Diachok, Dr. Budd B. Adams, and Dr. Ron Dicus for many helpful discussions, and to David Diehl for helping with the measurements and data processing.

REFERENCES

1. D. Ross, *Mechanics of Underwater Noise*, Pergamon Press (1976).
2. J. Cybulski, "Probable Origin of Measured Supertanker Radiated Noise Spectra," *Oceans 77 Conference Record*, 1, Institute of Electrical and Electronic Engineers, 15C/1-8, 1977.
3. H.W. Kutschale, "Rapid Computation of Wave Theory of Propagation Loss in the Arctic Ocean," Lamont-Doherty Geological Observations of Columbia Univ. Tech. Report No. 8, 1973.
4. L. Gray, and D. Greeley: "Source Level Model for Propeller Blade Rate Radiation for the World's Merchant Fleet," Technical Memorandum 458, Bolt, Beranek and Newman, Inc., Cambridge, Mass. 02138, 1978.
5. J.A. Shooter et al., "Characteristics of Ambient Noise in the Deep NW Pacific," ARL-TR-79-39, Applied Research Laboratories, POB 8029, Austin, Tex. 78712.
6. W.D. Mark, "Effects of Rotational Speed Fluctuations and Inflow Turbulence on Merchant Ship Propeller Cavitation Volume Spectra," Technical Memorandum #660, Bolt, Beranek and Newman, Inc., Jan. 1982.
7. Wright, E.B.: "Flow-Induced Noise in Merchant Ship Broadband Source Levels," *J. Acoust. Soc. Am.* 65(S1), S89(A).

Appendix A

OPERATIONAL CONDUCT OF EXPERIMENTS

Sensor Hydrophone and Environmental Constraints

Acoustic instrumentation was available in the form of AN/SSQ-57A (XN-5) sonobuoy, modified [A1] for very low frequency (VLF) response to 1 Hz with a 305 m hydrophone. This unit is air deployable from the NRL EP3A research aircraft. A deep hydrophone sensor was selected to receive signals uncontaminated by a bottom return for range separations as great as possible, to acquire reliable data approaching bow and stern ship aspect angles. However, the modification of the buoys was such that they were considered to be self-noise limiting at about sea state 3, generally characterized by whitecaps of 1.5 m wave height.

Thus, an important consideration was the daily Fleet Weather Center (FWC) forecast of wave height contours over the areas of interest. Personnel of FWC ROTA, Spain provided a real wave height 2 to 8 ft contours in 1 ft intervals. With this chart daily operations were logically restricted to those regions of a 3-ft wave height and less. Generally the prognostications were found to be accurate, although generally higher by about 1 ft.

Aircraft Platform—Typical Operations

Staging out of ROTA permits the aircraft to reach the farthest operating area selected with 2 hours transit. This allows 6 hours to search for ships, ships' screening and acceptance, rigging (ships' course, speed and photographs) and acoustic data acquisition procedures before a transit back to base while maintaining flexibility as to alternate landing fields. The Litton Inertial Navigation System (INS) aboard an aircraft was to be the primary navigational instrument. During the transit to the shipping lane in the area, a calibration is made of the analog and digital systems employing CW tones and a random noise generator with a transmitter test set. After reaching the shipping lane, a search either to the north or south is made. After an acceptable vessel is found it is rigged and at least four mark-on-tops (MOT) are taken over a 30 min period to establish course and speed. A check has been made for proximity of other ships to try to maintain a separation of 10 to 15 nmi at the estimated CPA to sensor deployment. During this period a photograph abeam and astern is taken and an aircraft expendable bathythermograph (AXBT) drop is made. The navigator dead-reckons an INS position approximately 45 min ahead of the ship, and the sonobuoy deployment run begins from a point 10 nmi perpendicular to the track at an altitude of 91 m and a speed of 180 knots. Five buoys are dropped at 10-s intervals (0.5 nmi spacing) with the initial buoy scheduled 1 nmi off the ship's course. After deployment, additional MOTs are taken and several passes made over the buoy line using the on-top-position-indicator (OTPI) to maintain a DRT plotter.

Instrumentation

The aircraft contains all of the instrumentation for reception, monitoring, analog recording and calibration. The output of the conventional sonobuoy receivers (ARR-52) down to 2 Hz was obtained by using the discriminator output jack. Spectral estimates in the 0 to 20-Hz and 0 to 500-Hz bands were made on-line by using a (UA 500) spectrum analyzer. A broadband (0 to 400 Hz) strip chart recorder provided additional monitoring of tape-recorded signals including a time code and a reference frequency. The primary processing was done on-line where the received signals from five sensors were sampled, held and multiplexed for simultaneous A-D conversion of the input into a Fourier analyzer.

WRIGHT AND CYBULSKI

This system [A2] was under control of a (HP21005) computer which also accepted the INS data. The thermal structure to 305 m was available from AXBT chart records made during each deployment.

REFERENCES

- A1. Ricalzone, L.C. and J.R. McGrath: "Modification of the AN/SSQ-57A (XN-5) Sonobuoy for VLF Applications," *J. Acoust. Soc. Am.* **60**, 1414-1416 (1976).
- A2. Steiger, D. and J.D. Clamons: "NRL's Oceanographic Computer System: Present Capability and Future Enhancements," NRL Memorandum Report 3216, 1976.

Appendix B
SHIP PHOTOGRAPHS



Fig. B1 — Belcargó

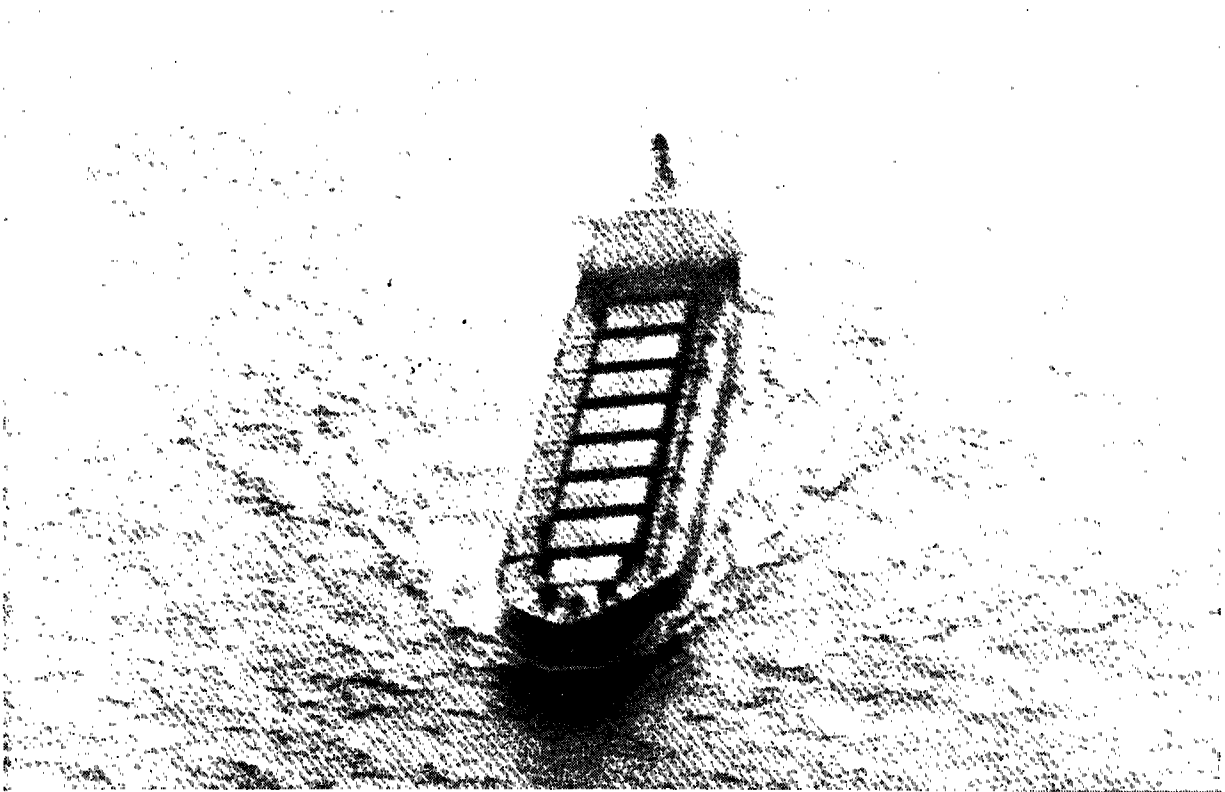


Fig. B2 — Belcargó

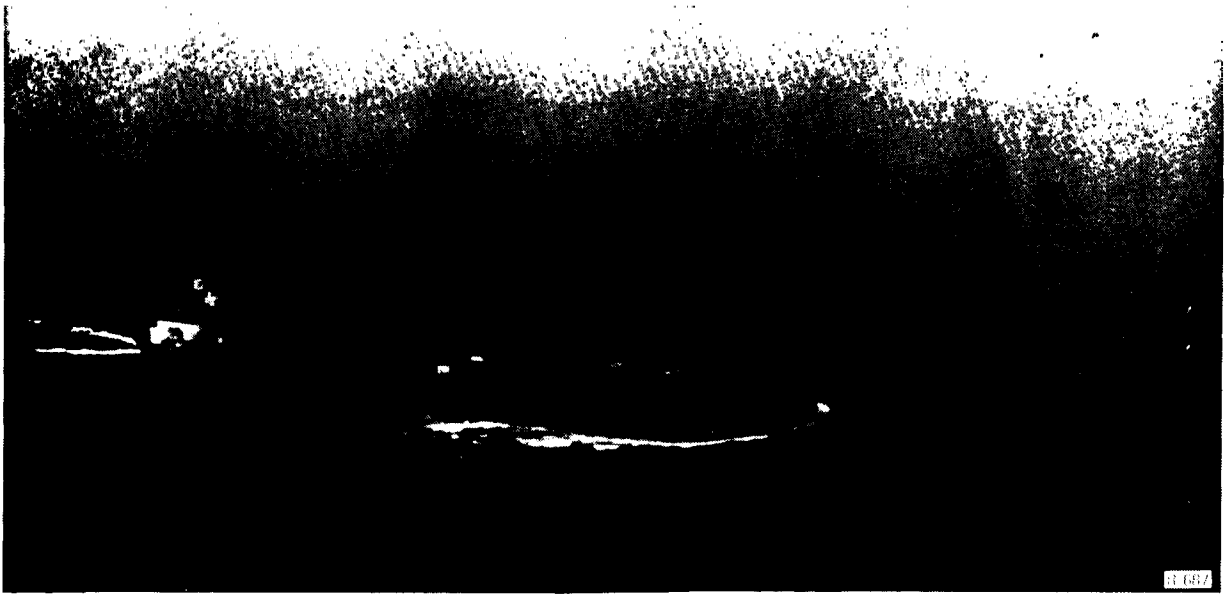


Fig. B3 — Esso Kagoshima



Fig. B4 — Esso Kagoshima

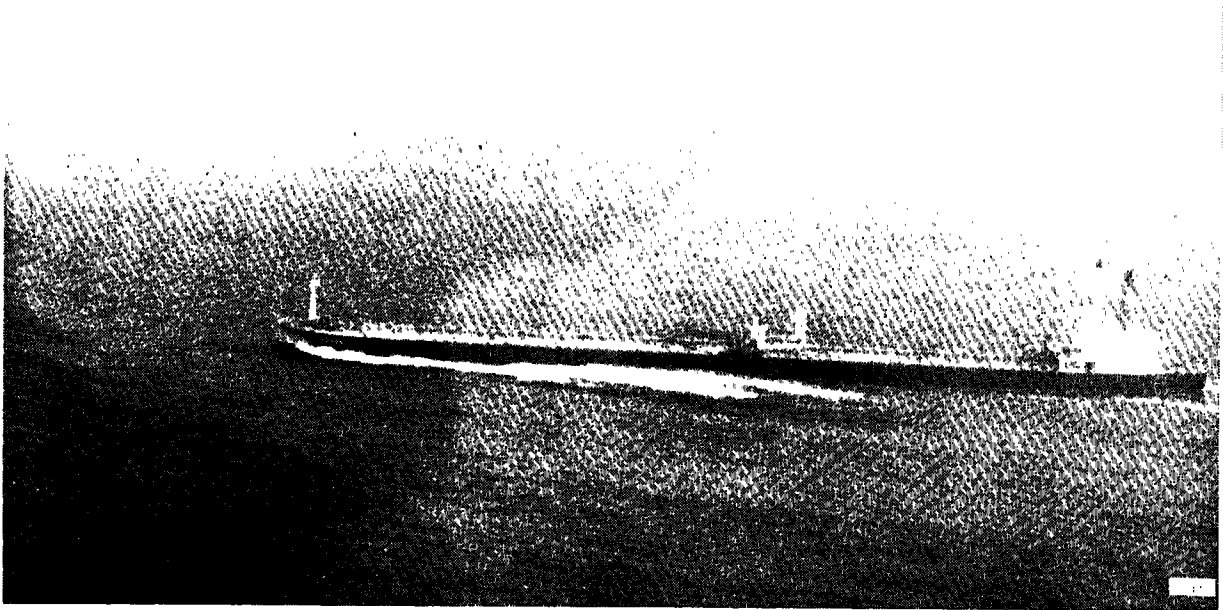


Fig. B5 — Lagena

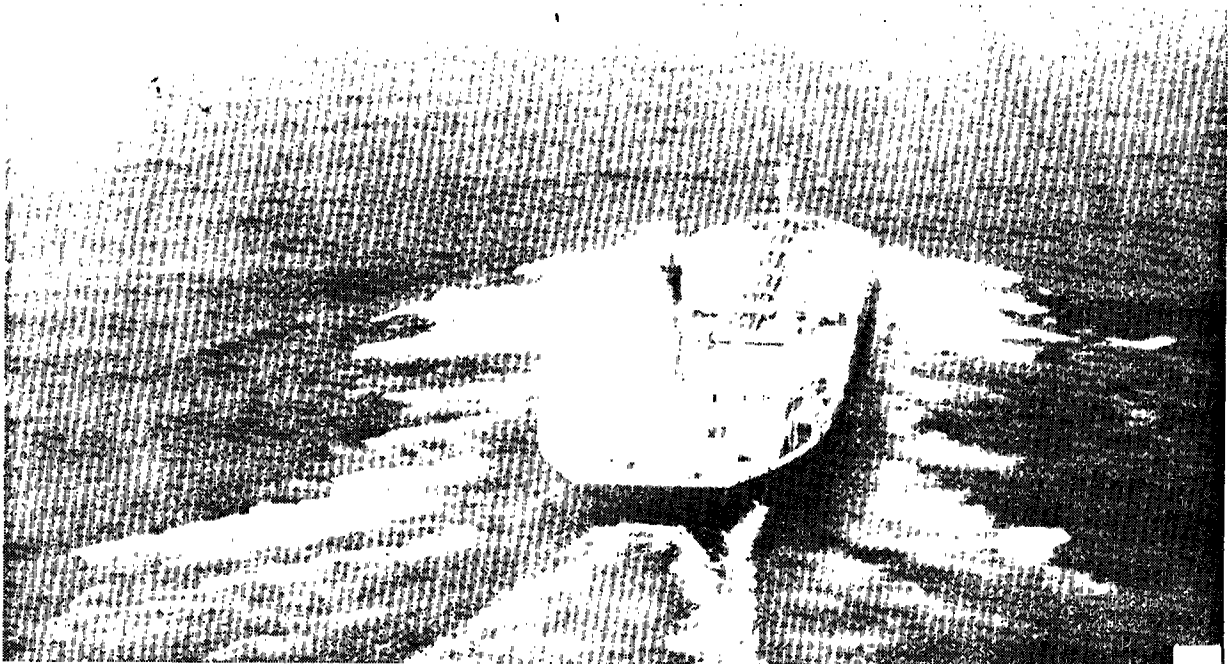


Fig. B6 — Lagena



Fig. B7 — Mostoles



Fig. B8 — Takara



Fig. B9 — Takara



R. 682

Fig. B10 — Thor



R. 683

Fig. B11 — Thor

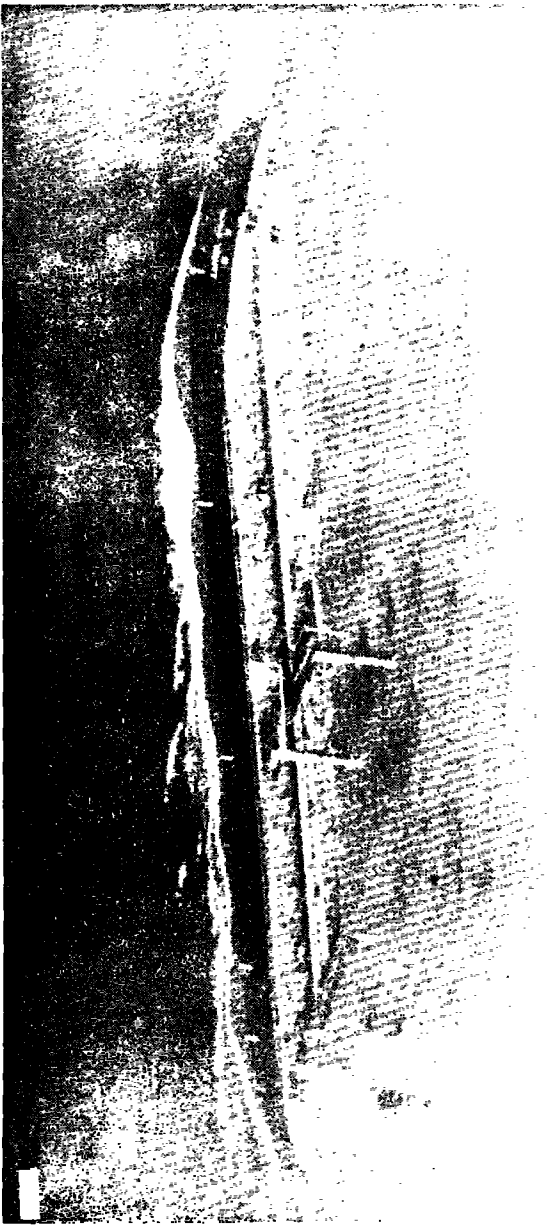


Fig. B12 — World Dignity

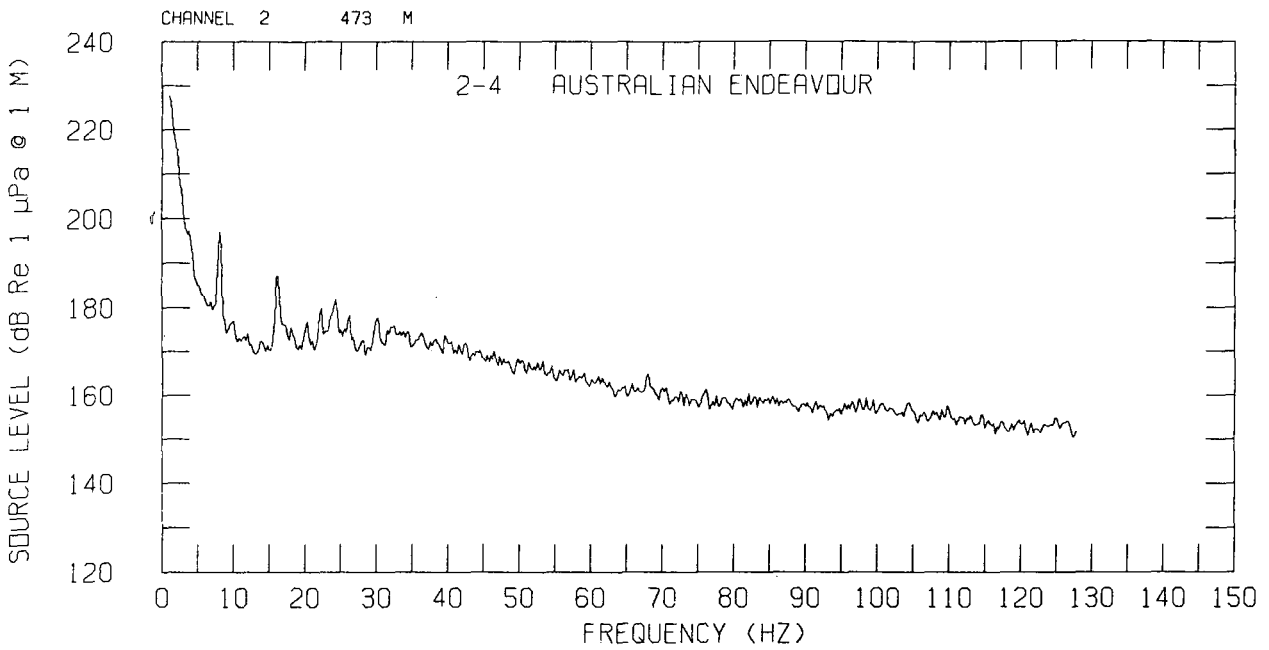
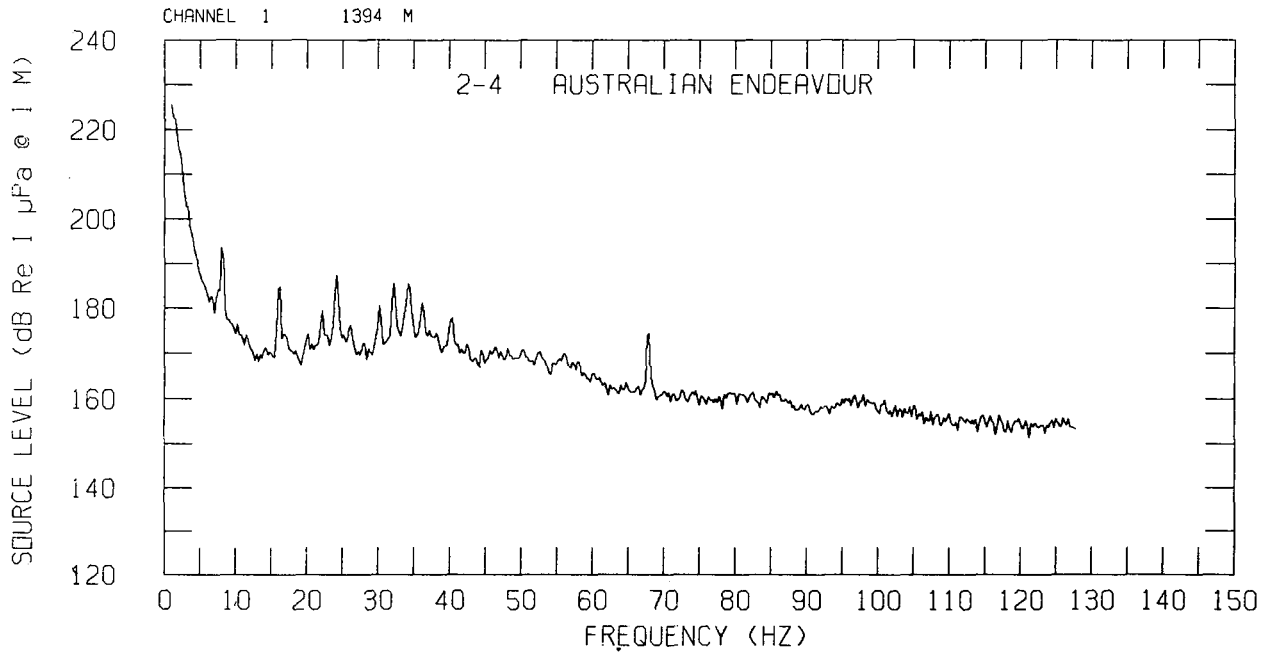


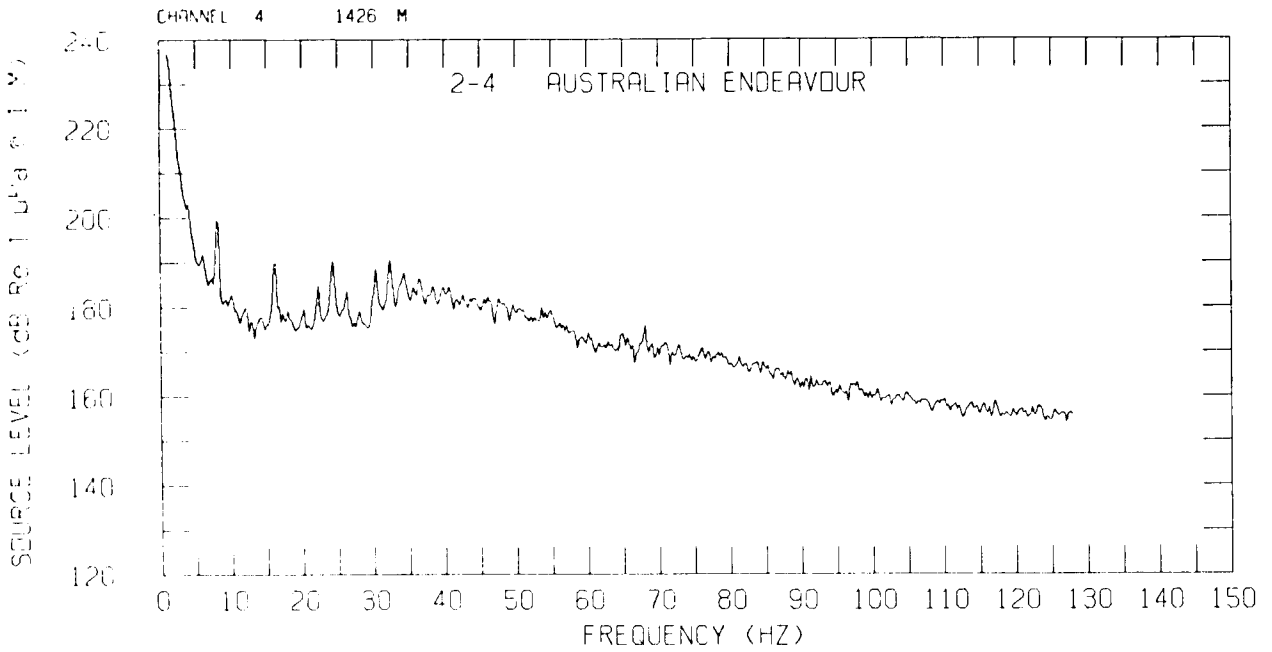
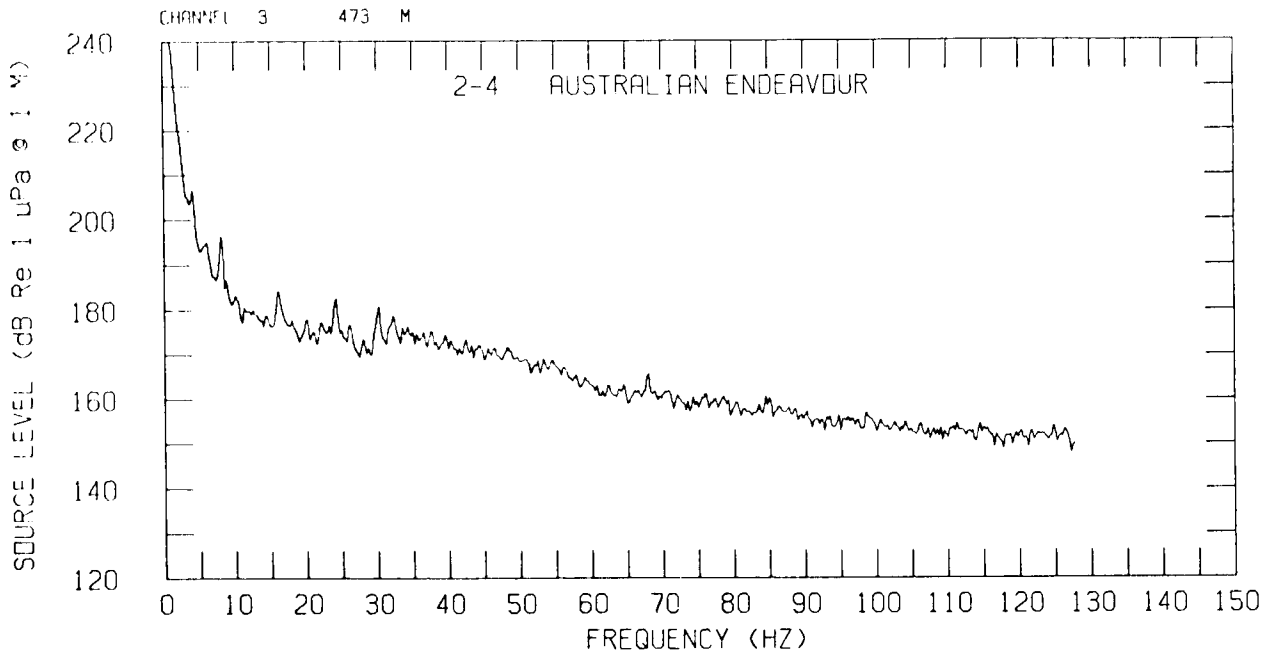
Fig. B13 — World Dignity

Appendix C
MEASURED SOURCE-LEVEL SPECTRA

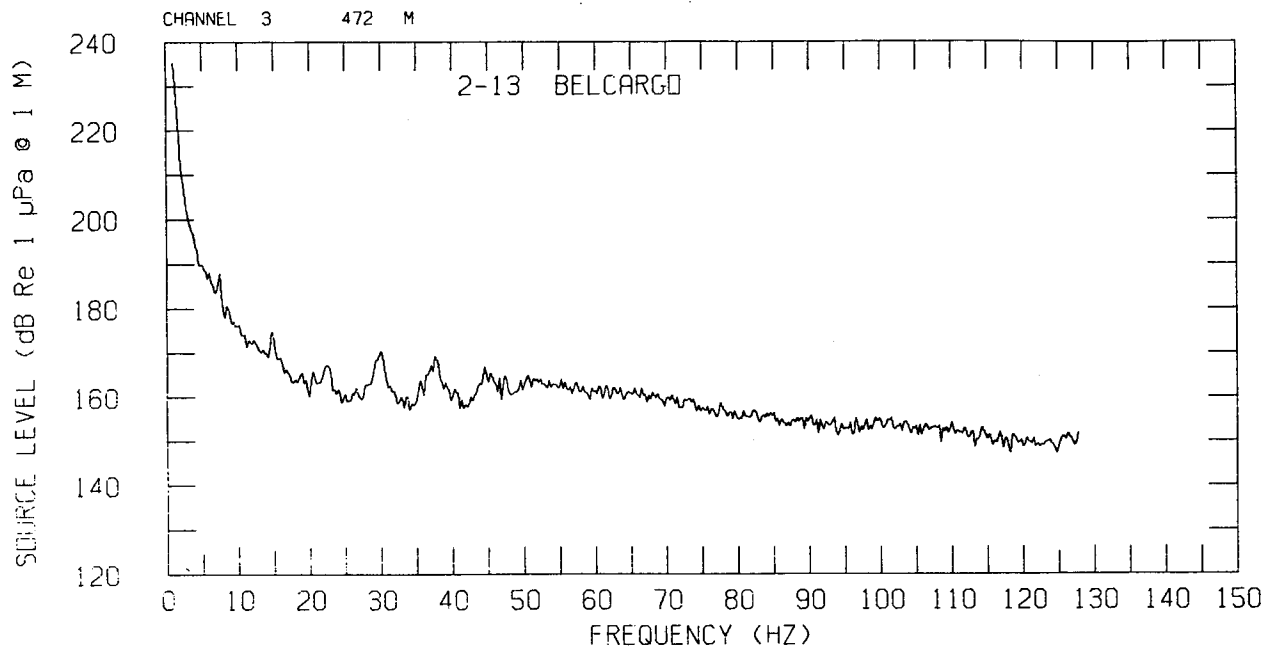
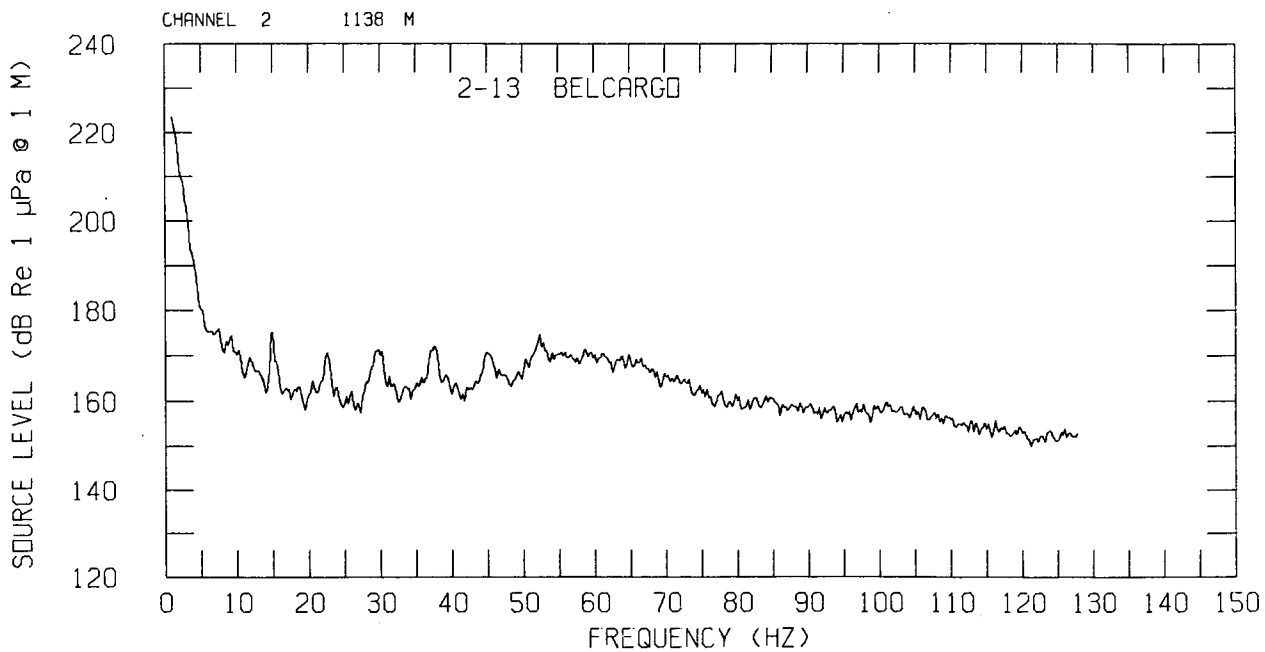
This set of source-level curves includes all usable measured spectra with CPA ranges in the 200-1300-in. window mentioned in the text. The CPA range appears above each plot. The hyphenated number preceding each ship name is the phase/run number.

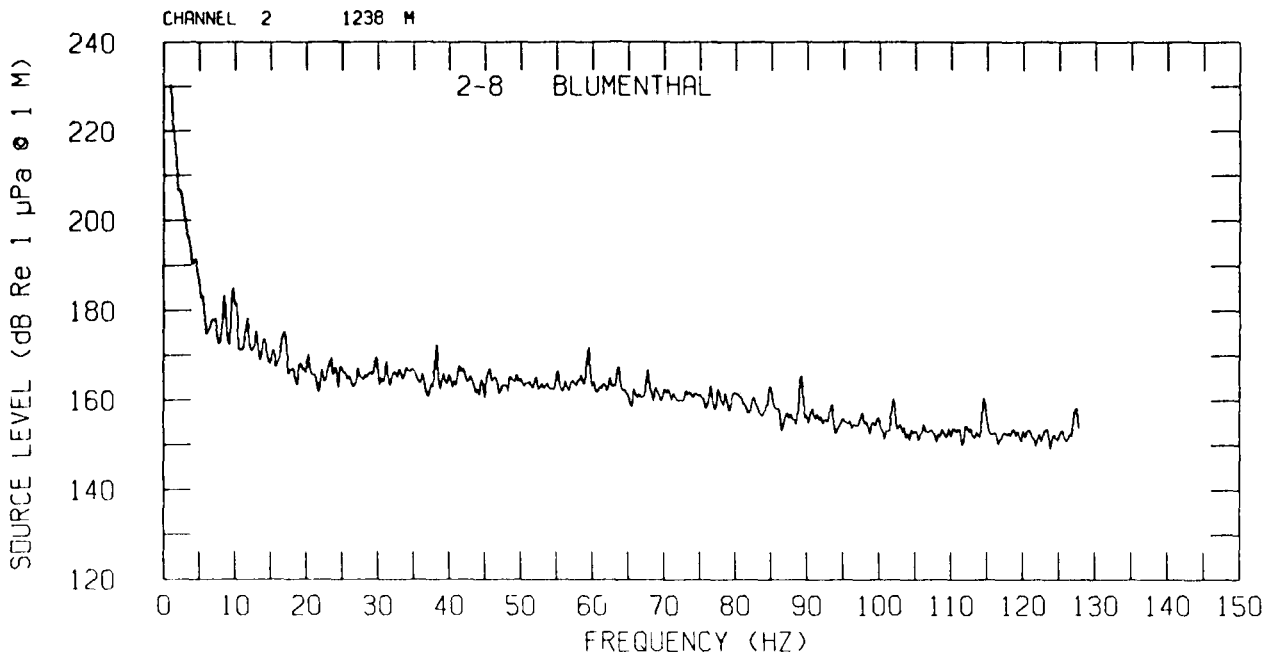
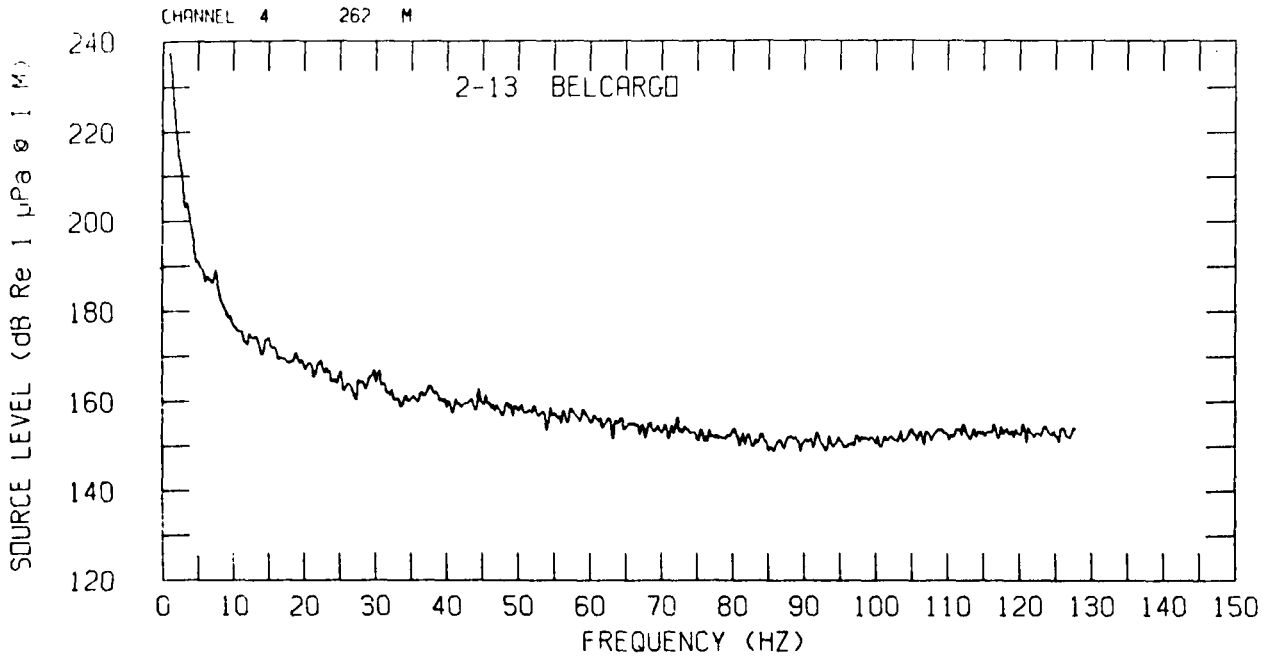
WRIGHT AND CYBULSKI



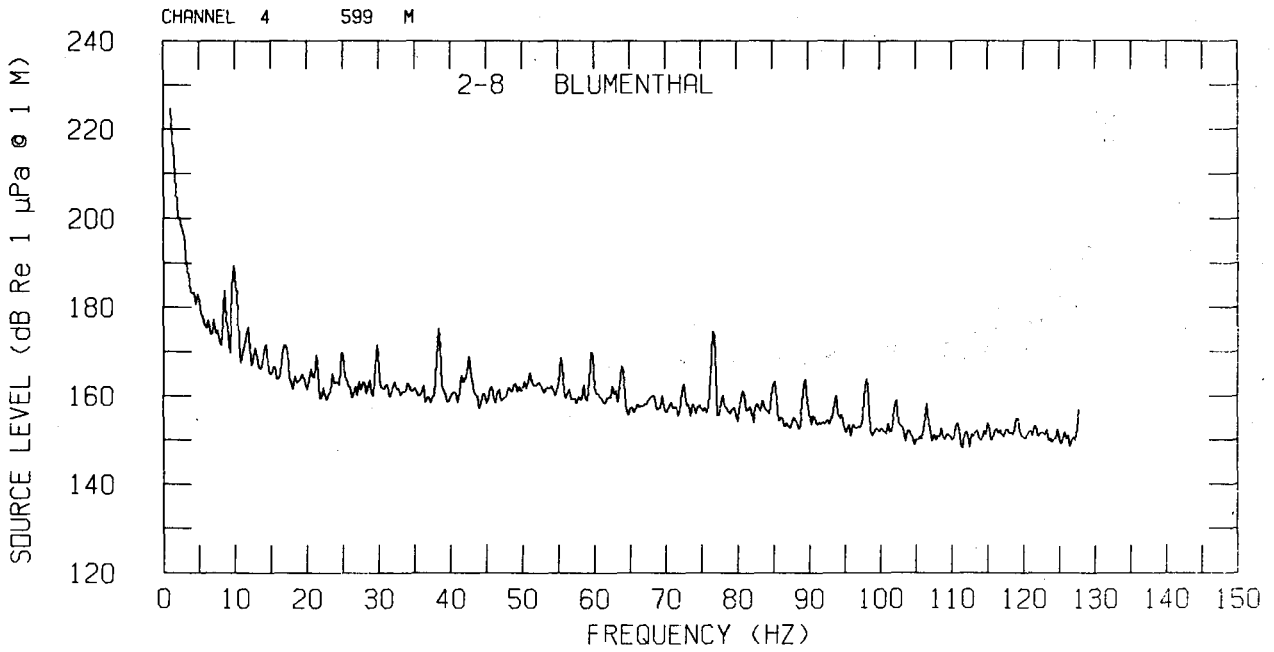
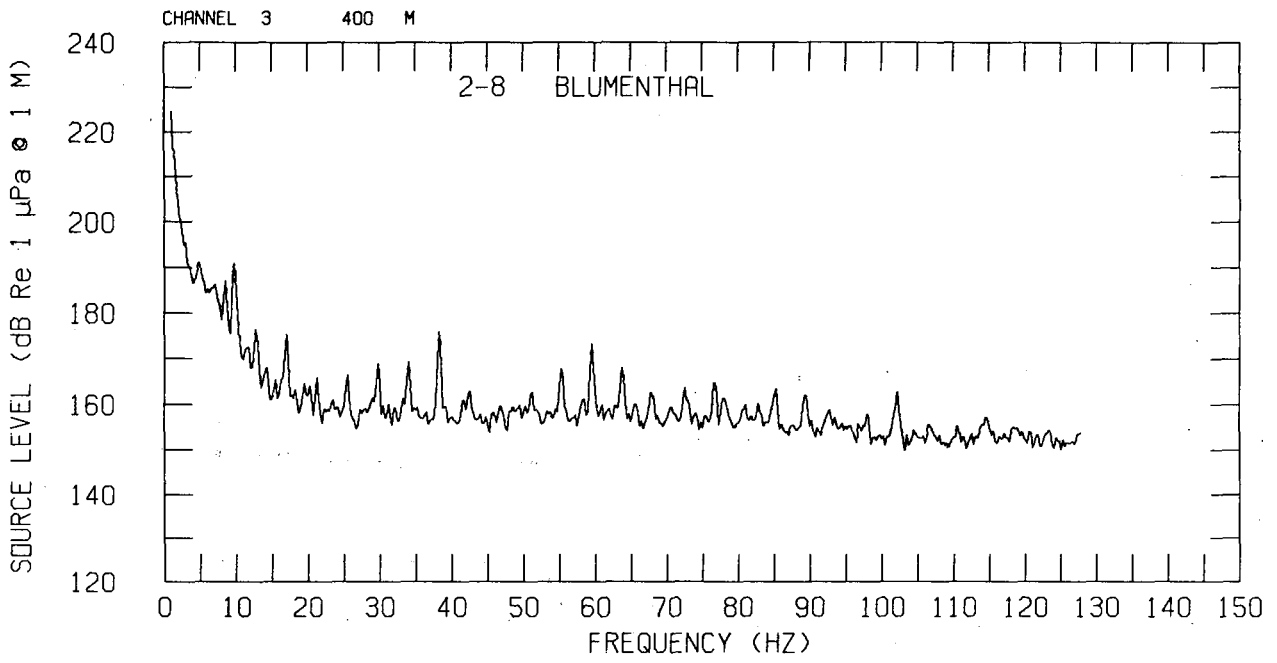


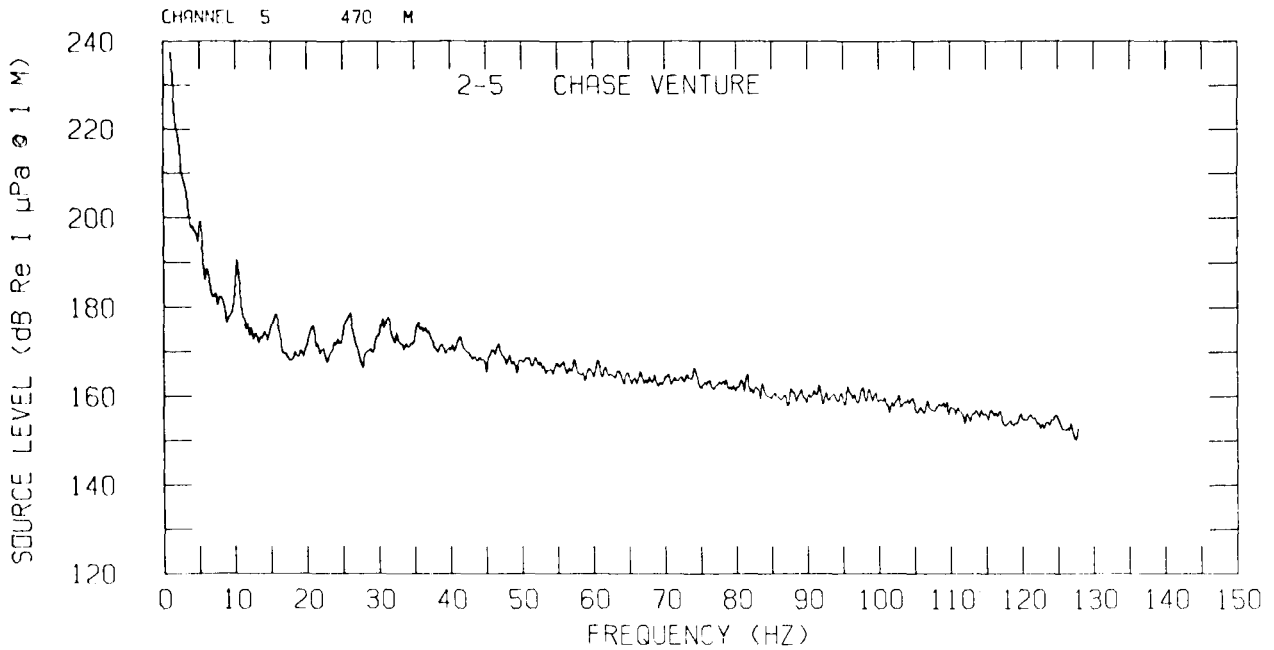
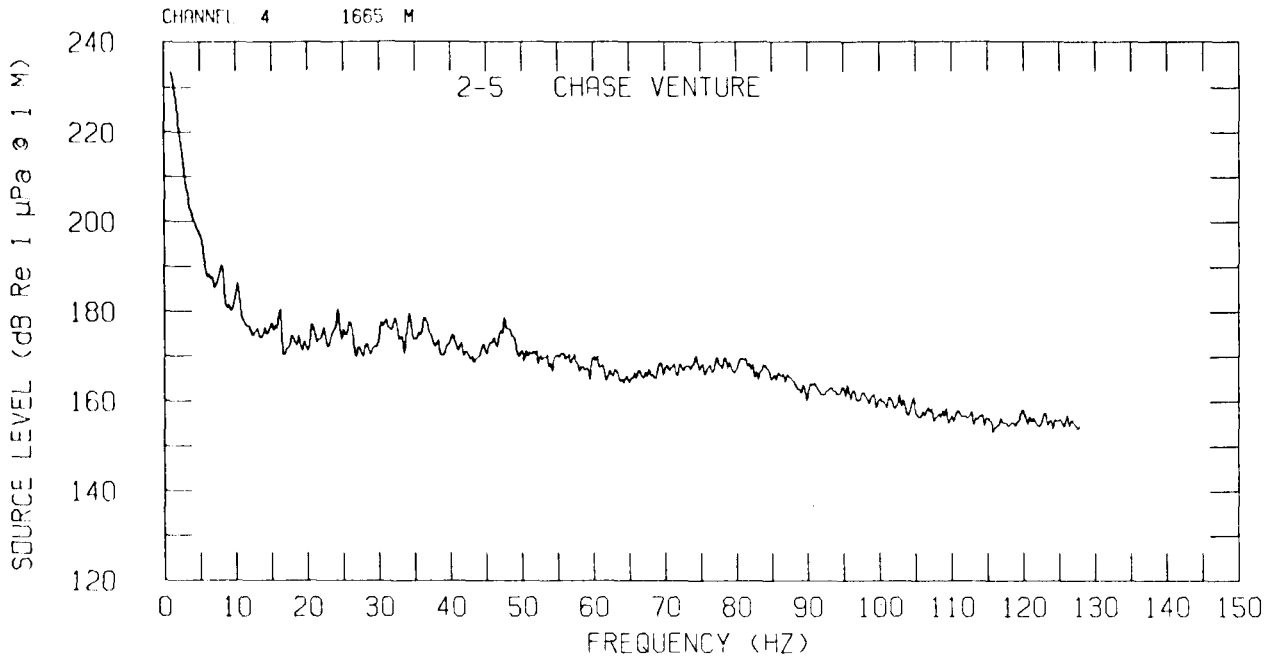
WRIGHT AND CYBULSKI



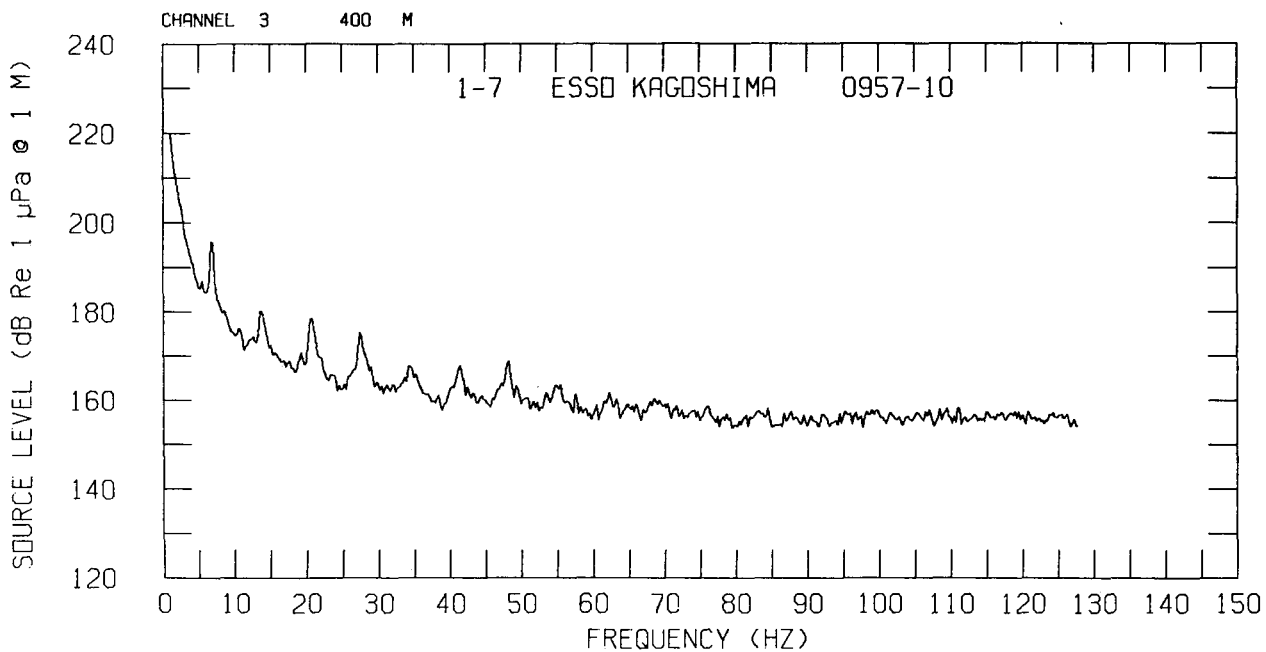
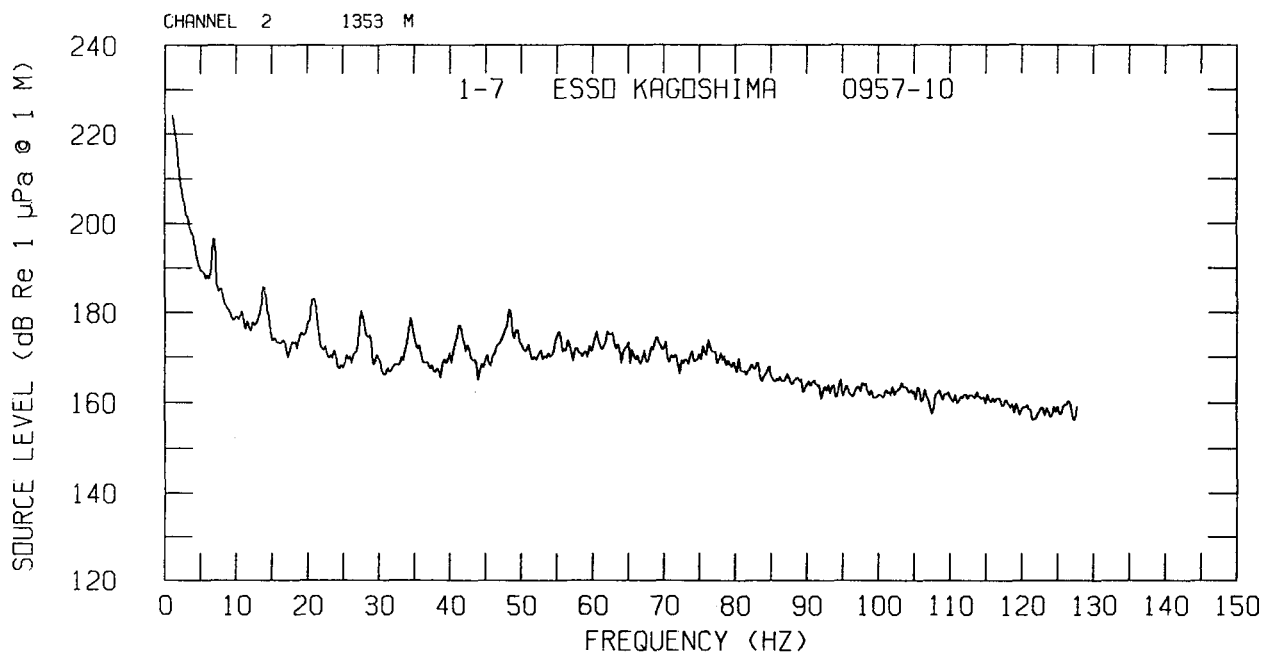


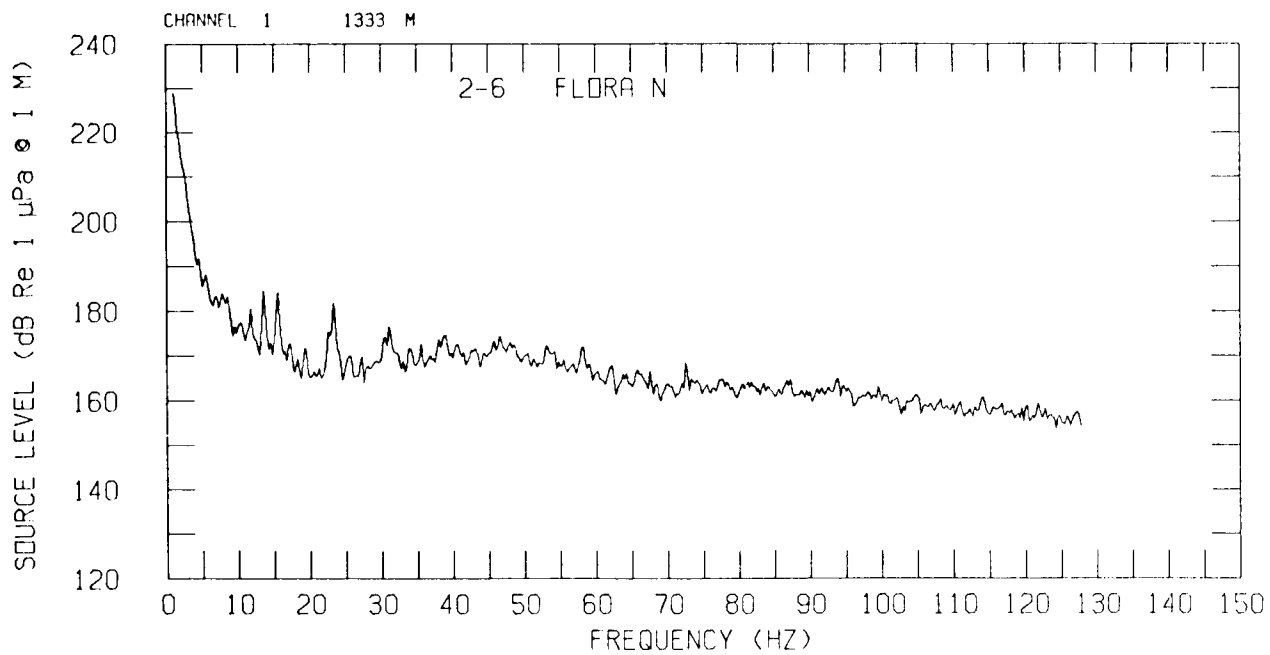
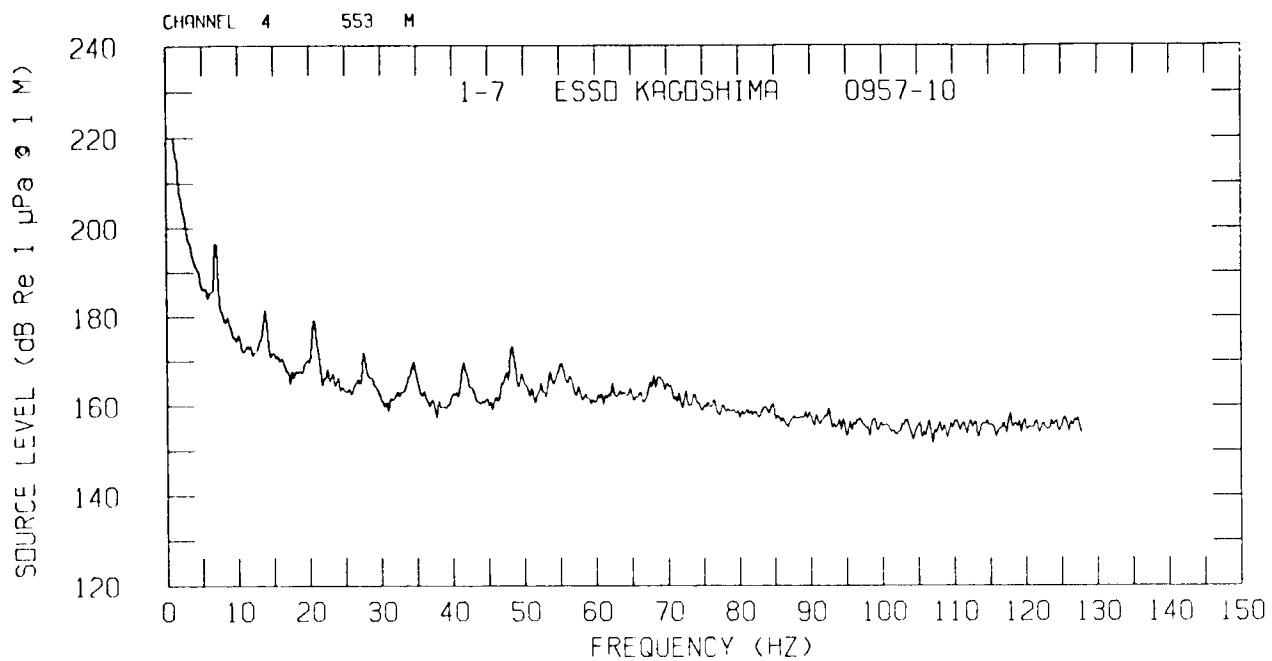
WRIGHT AND CYBULSKI



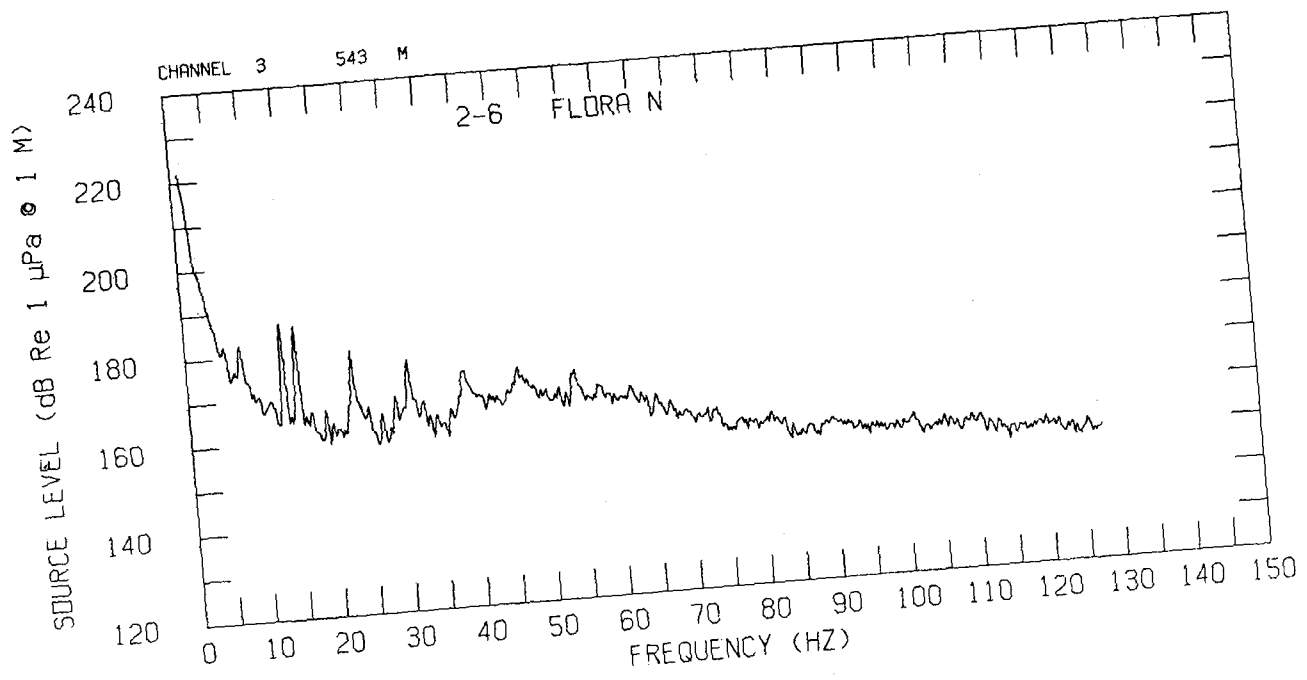
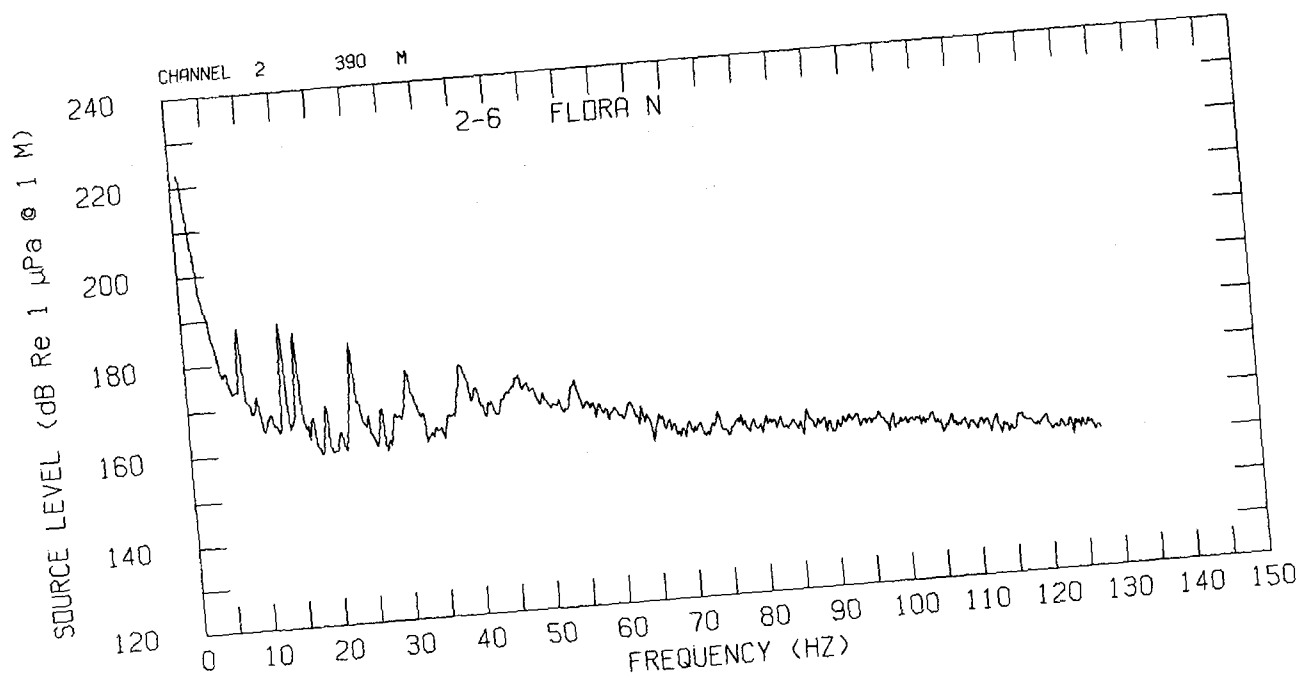


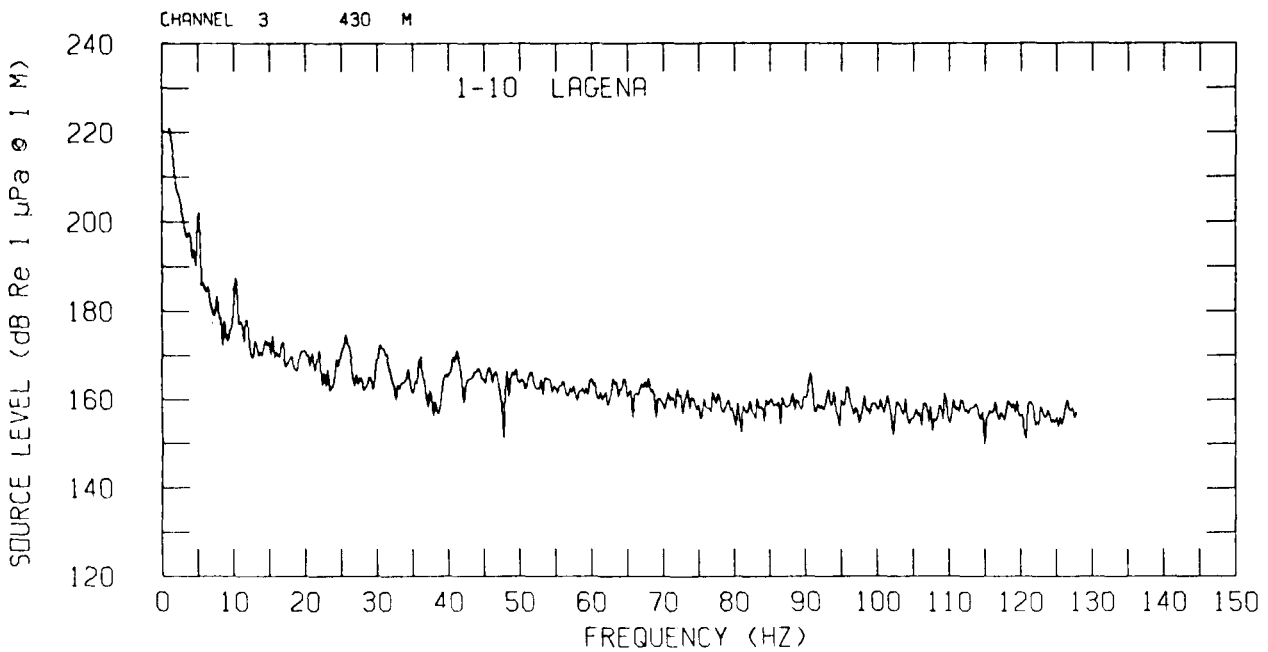
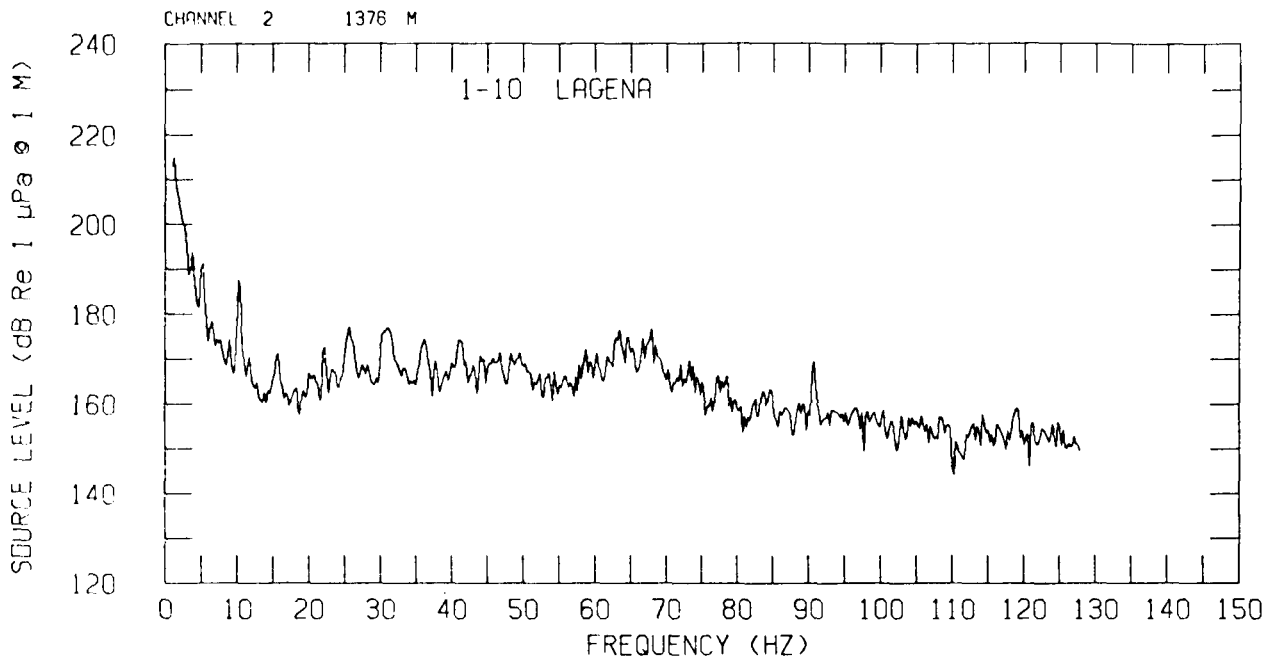
WRIGHT AND CYBULSKI



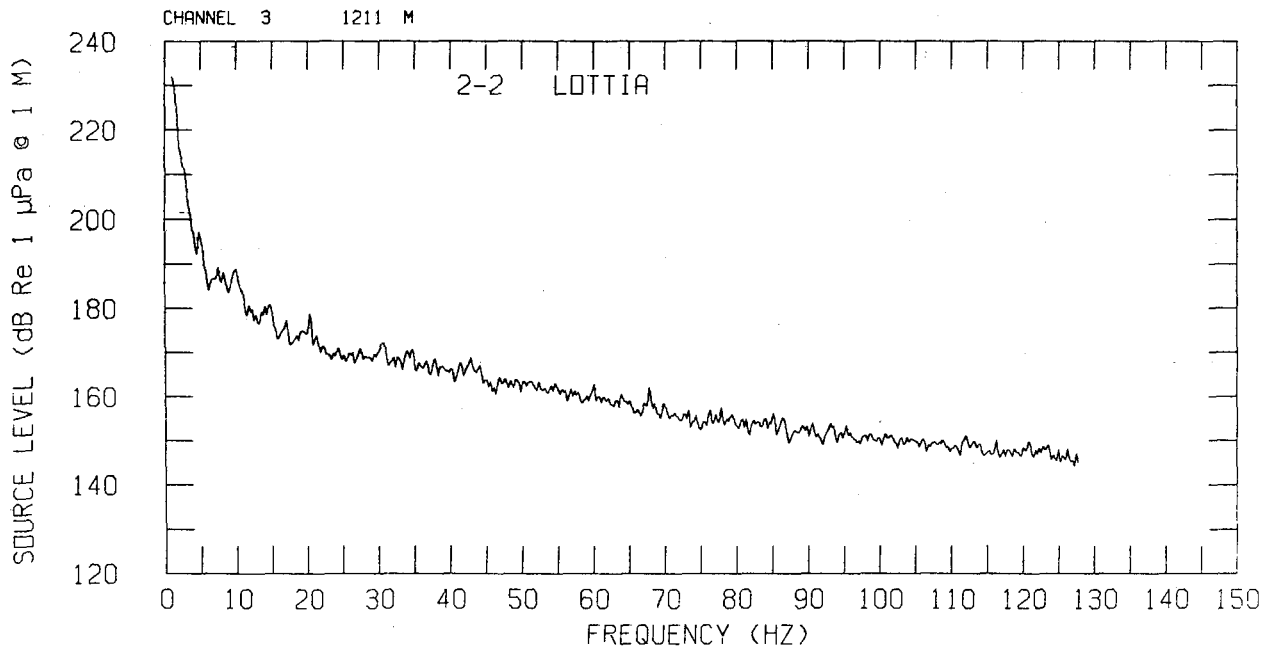
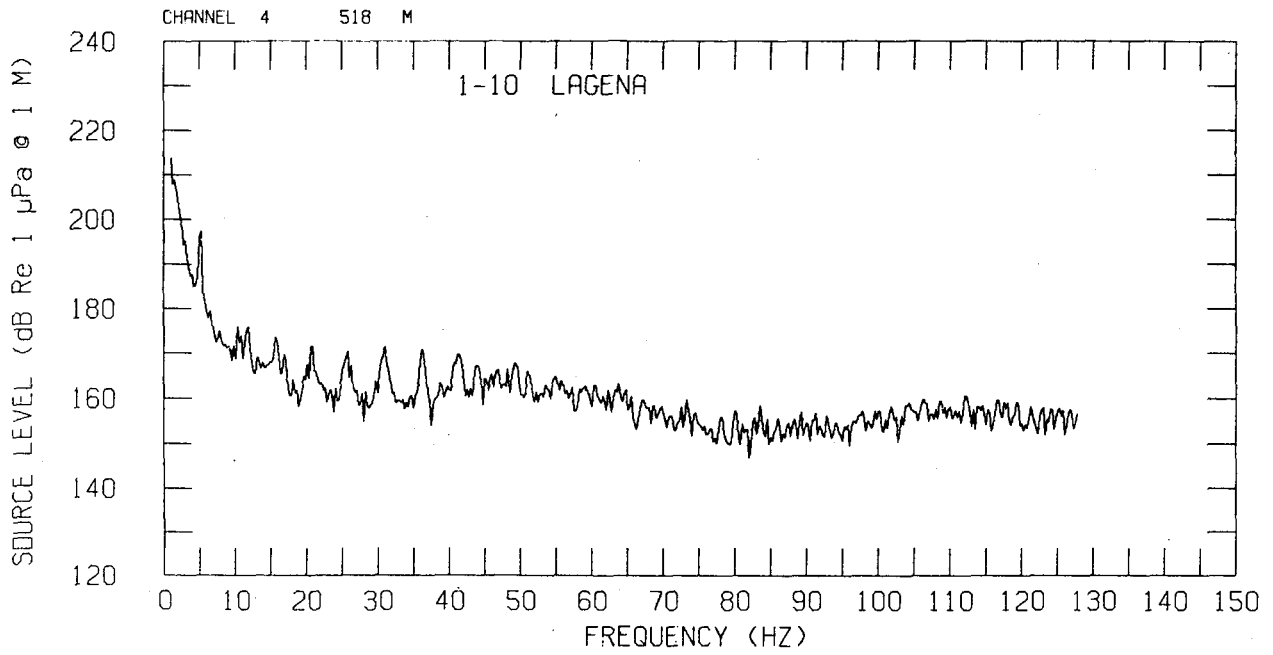


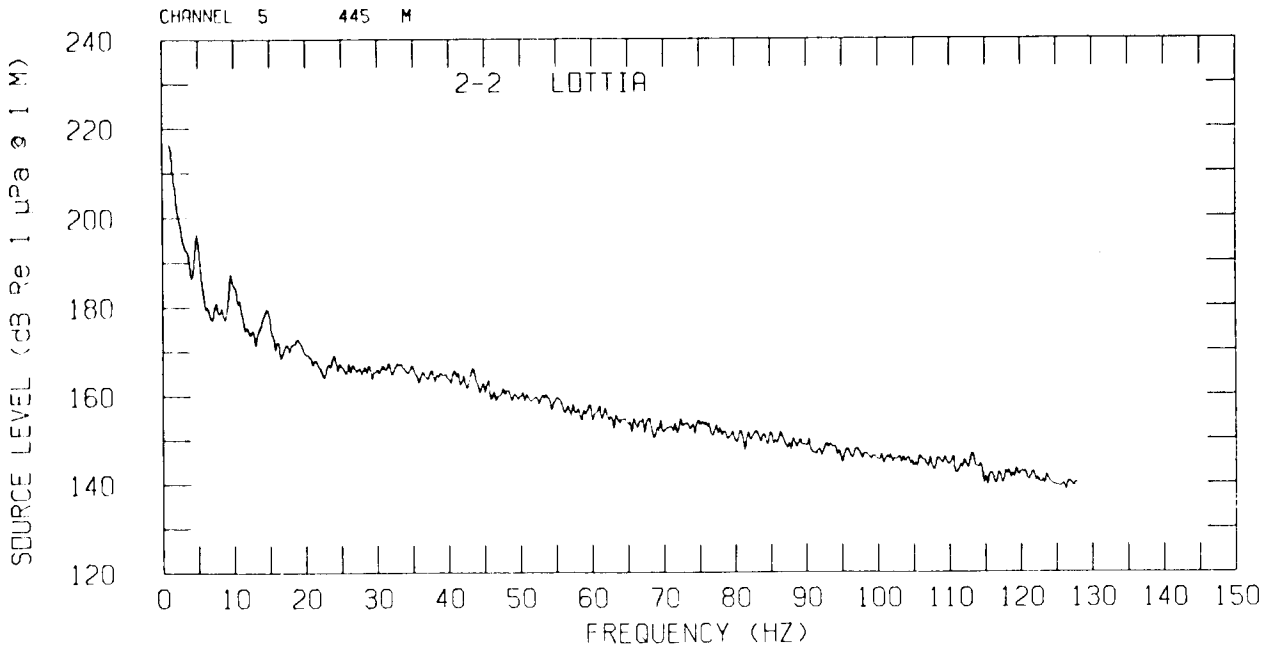
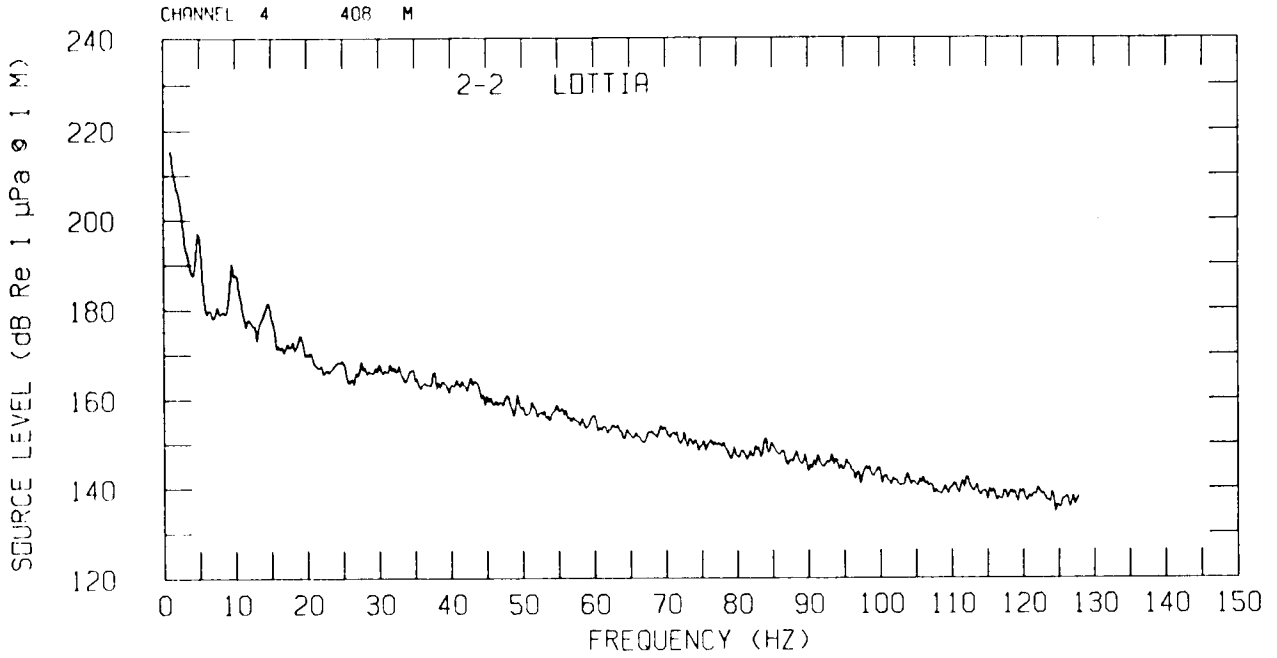
WRIGHT AND CYBULSKI



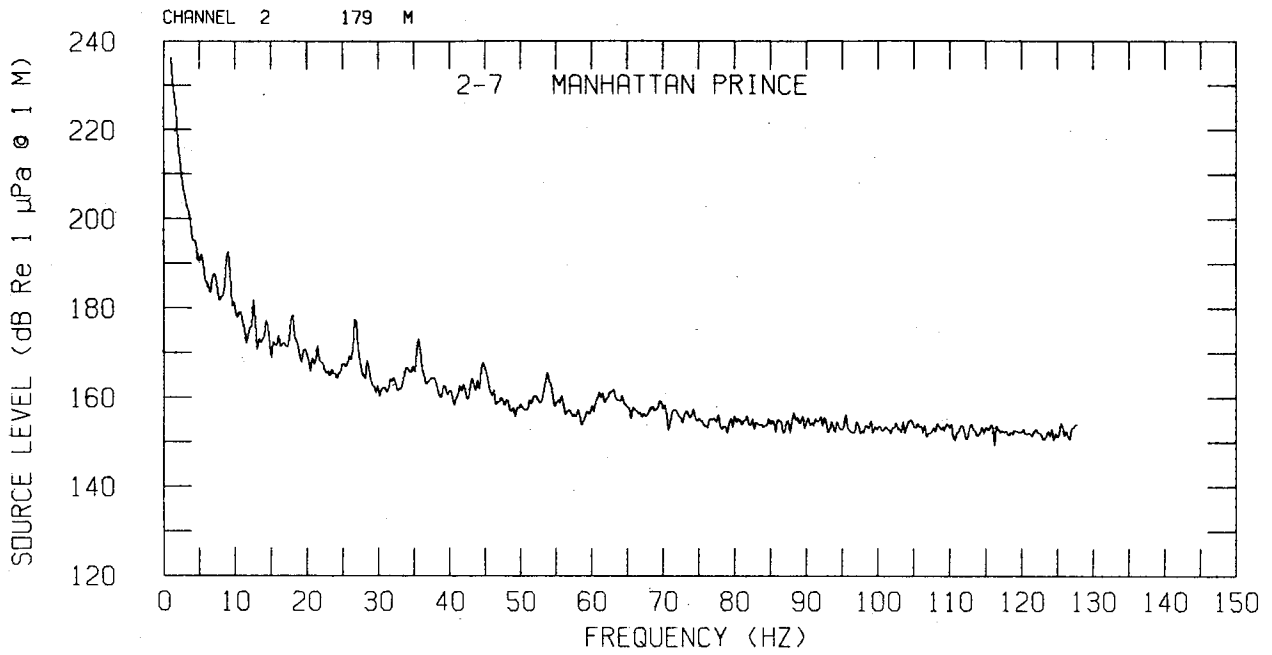
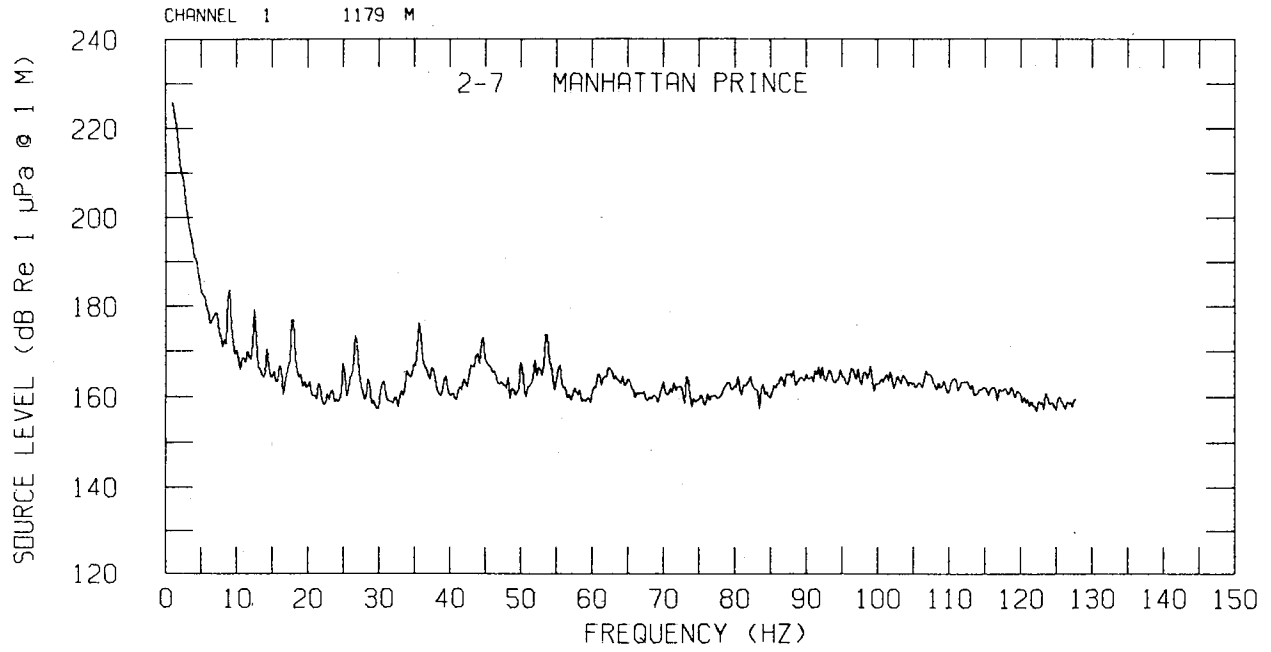


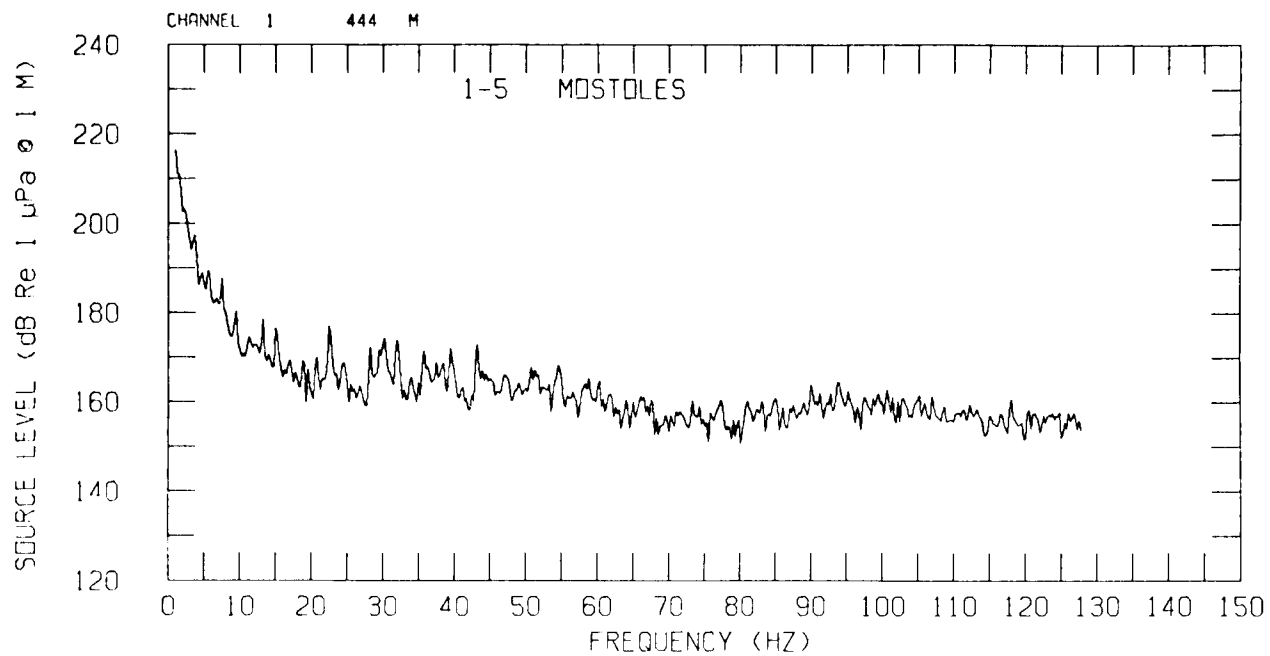
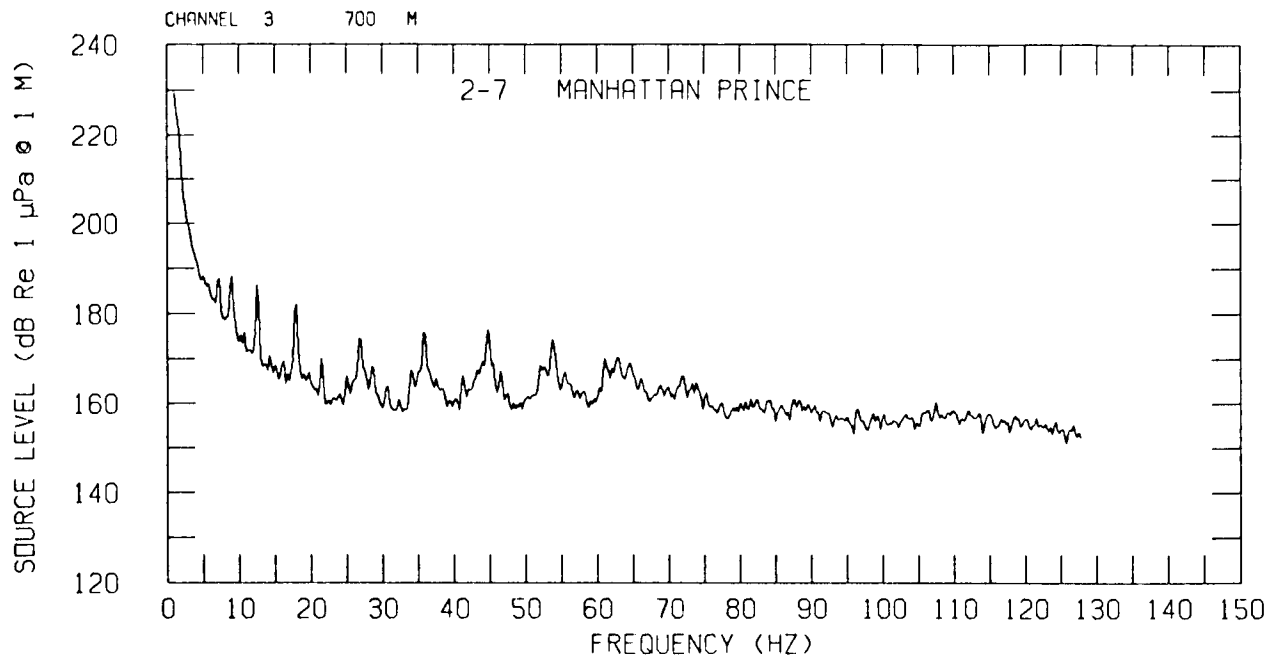
WRIGHT AND CYBULSKI



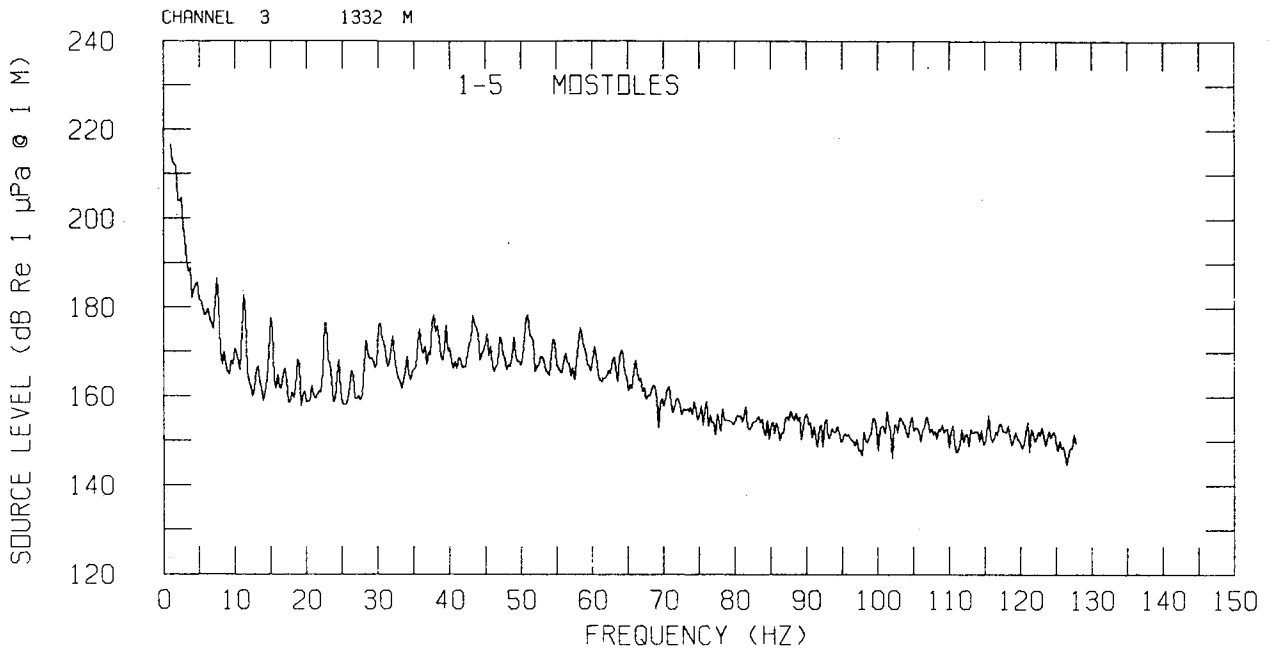
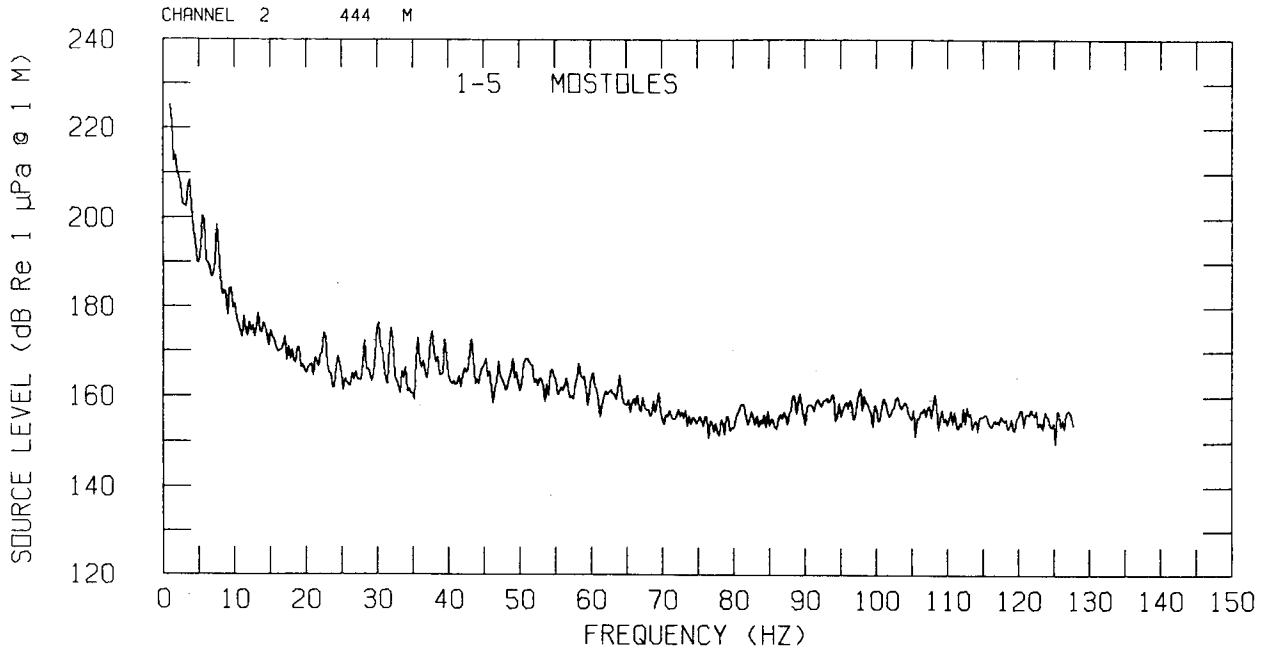


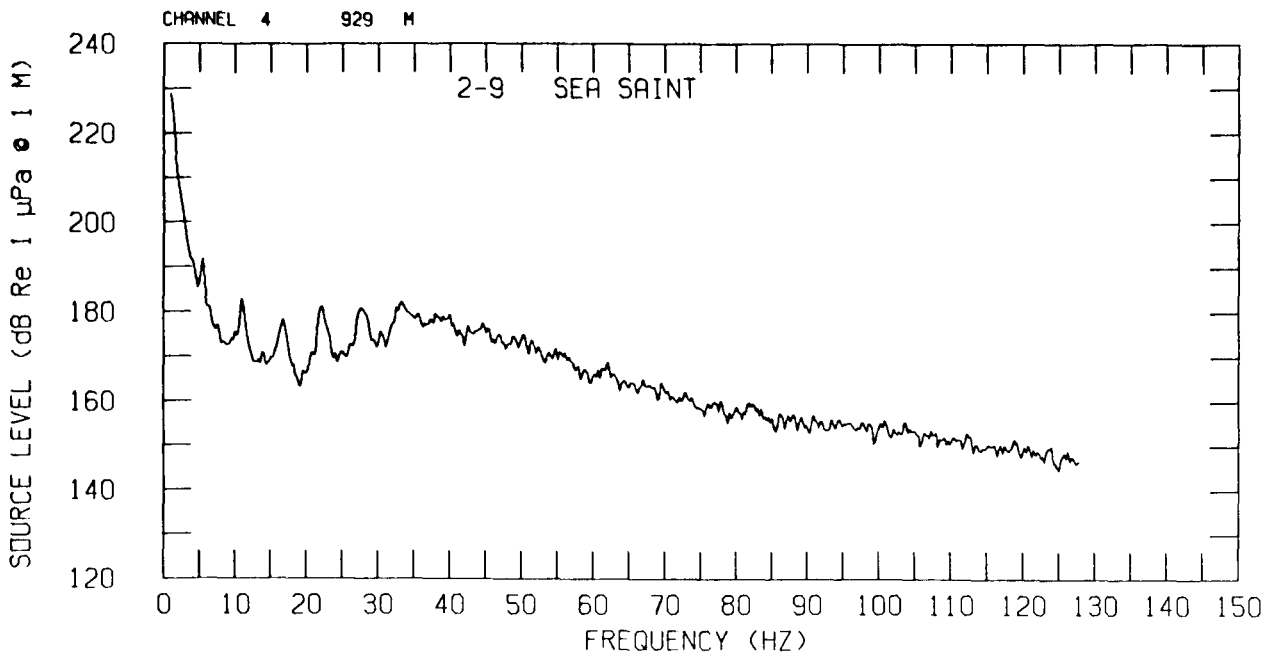
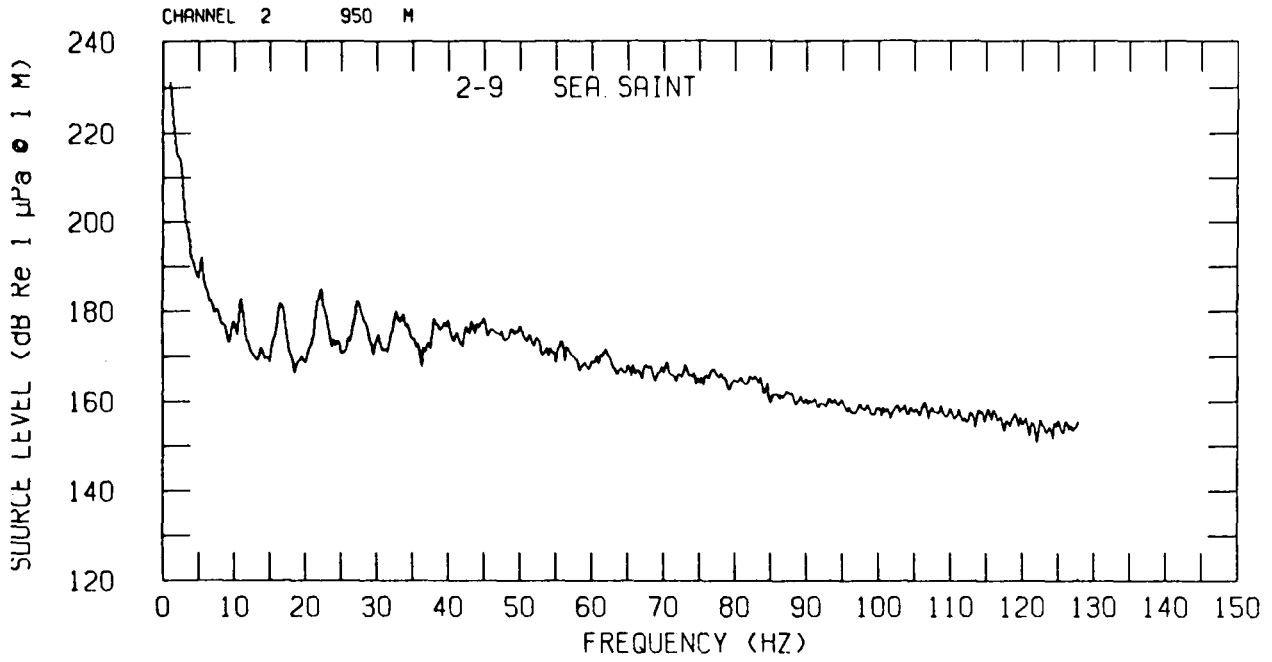
WRIGHT AND CYBULSKI



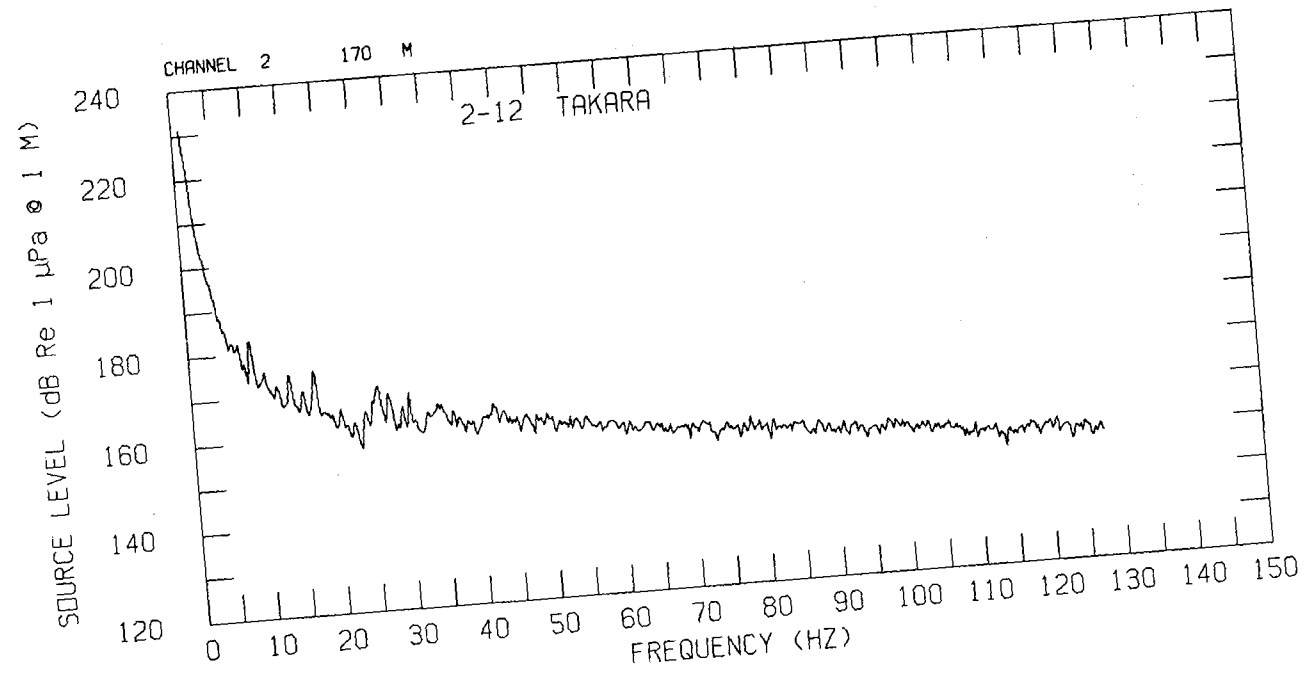
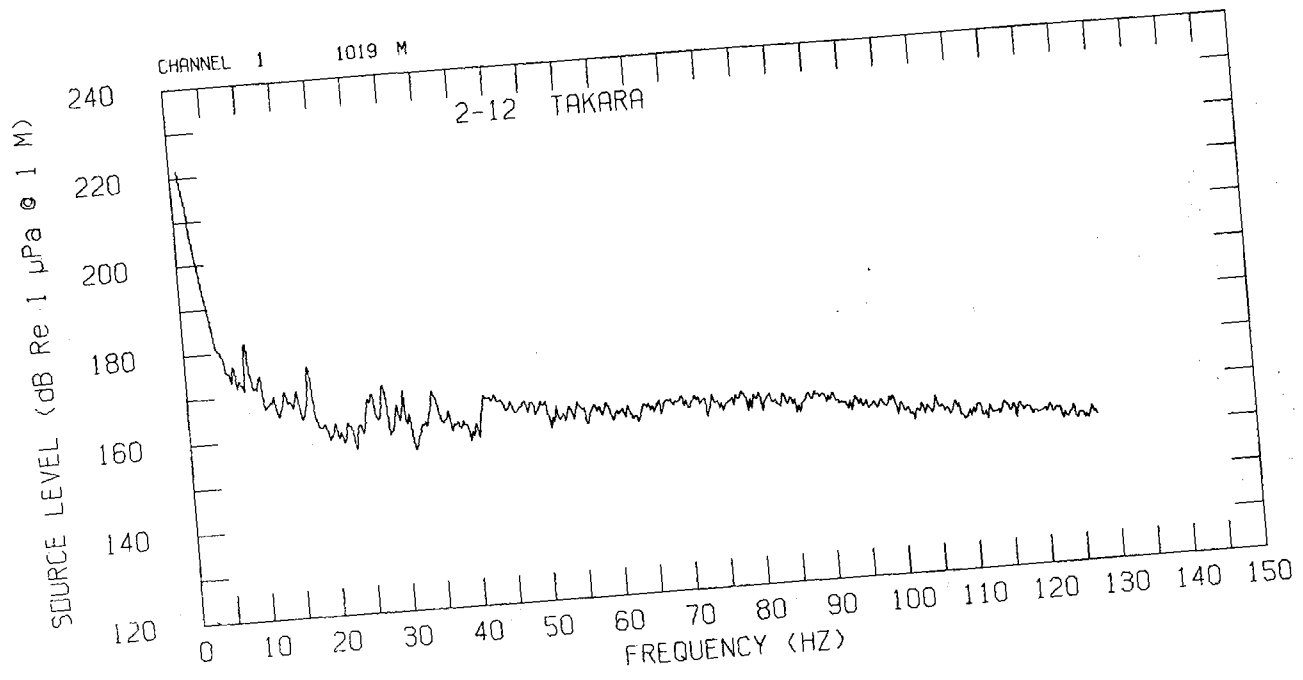


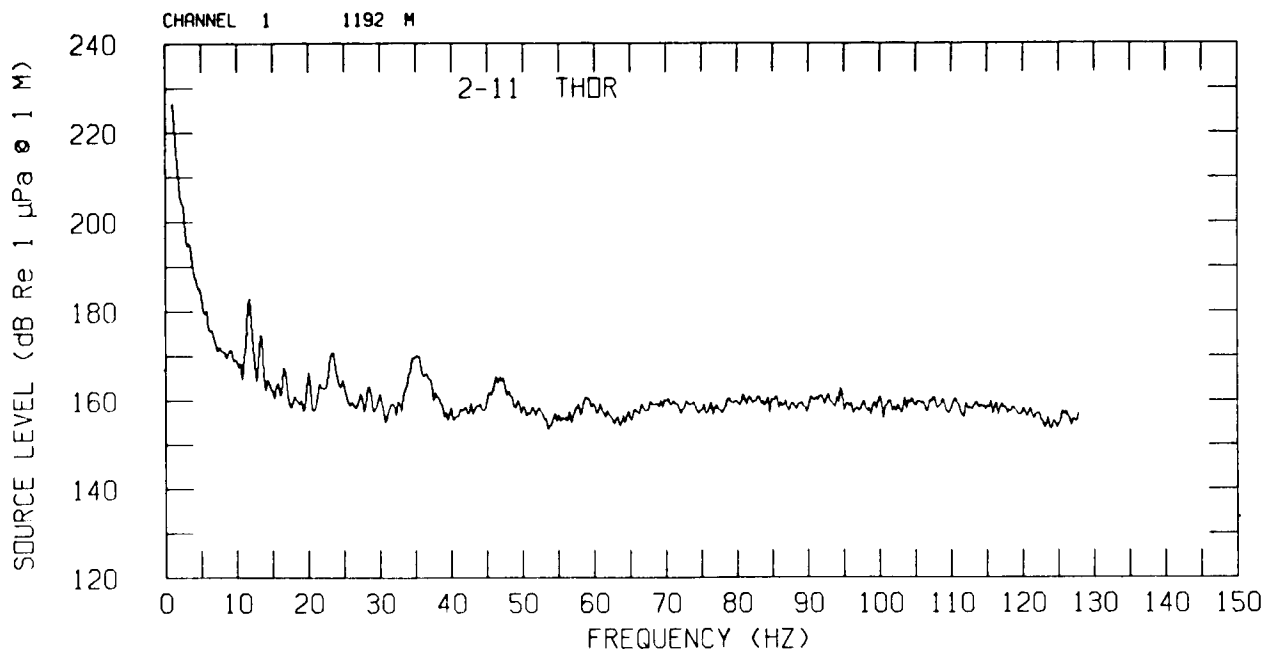
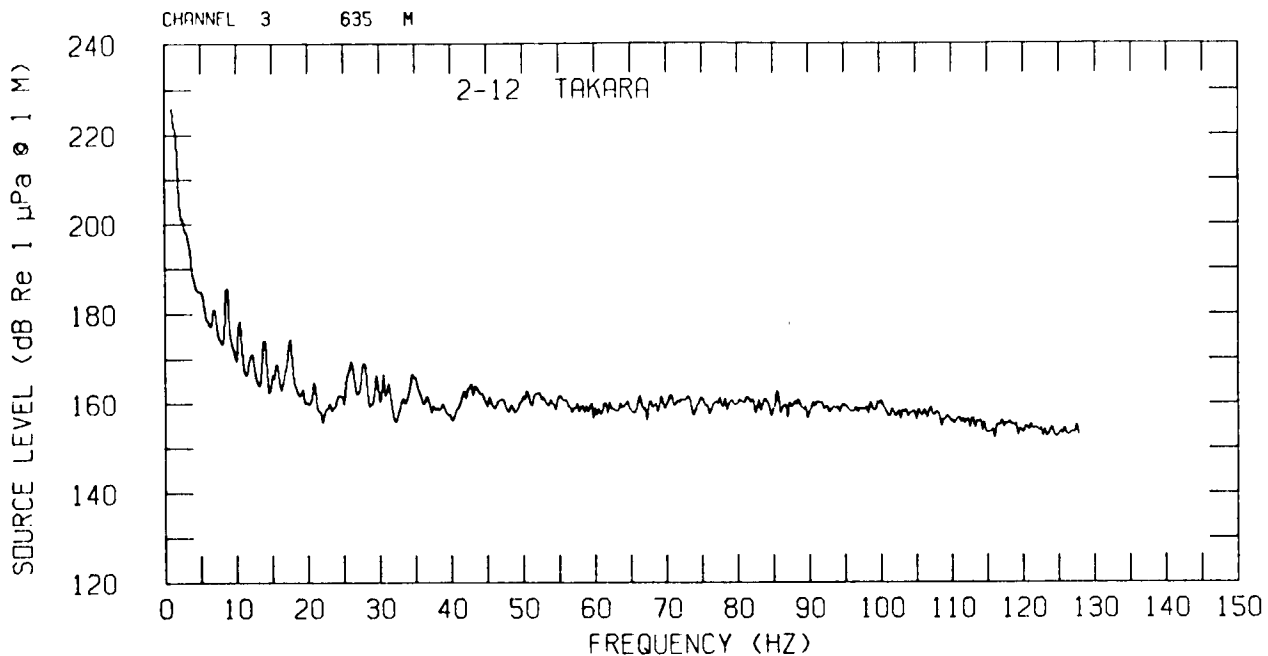
WRIGHT AND CYBULSKI



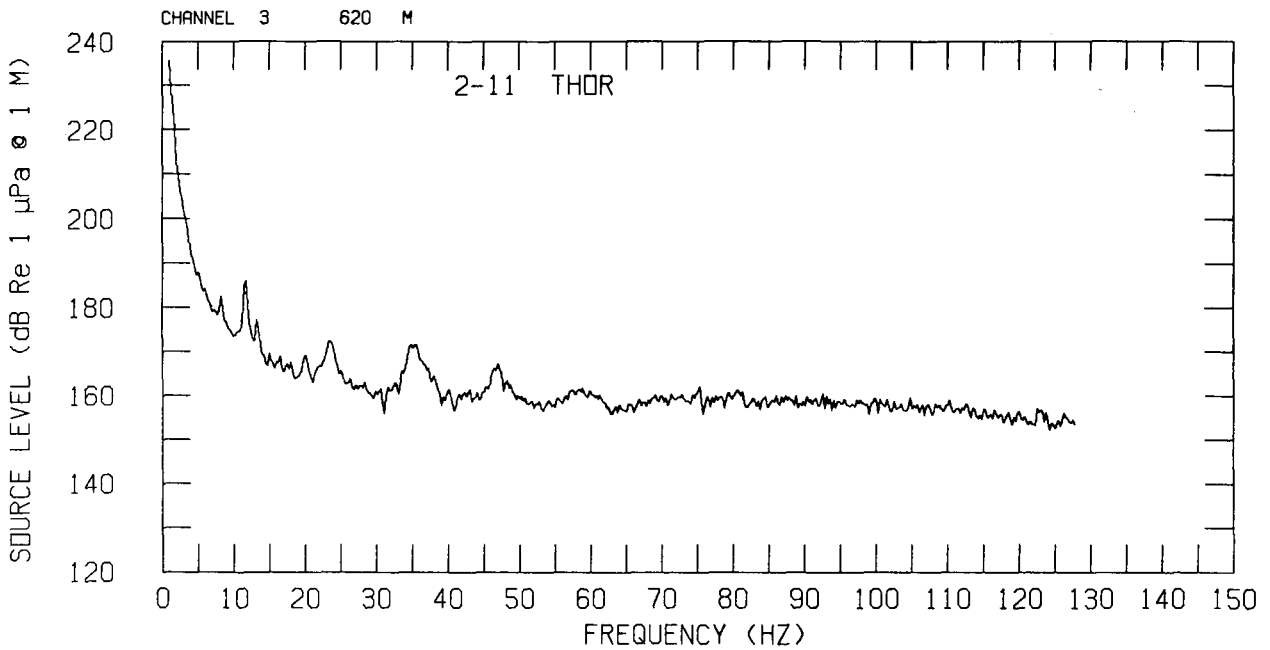
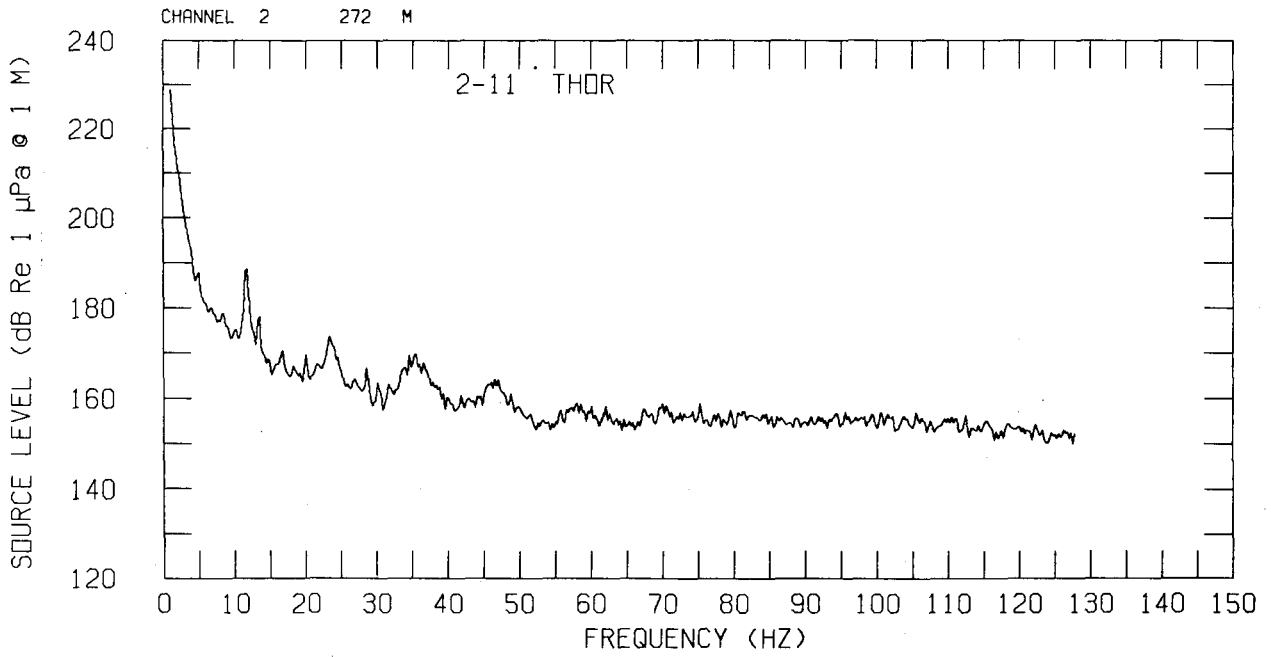


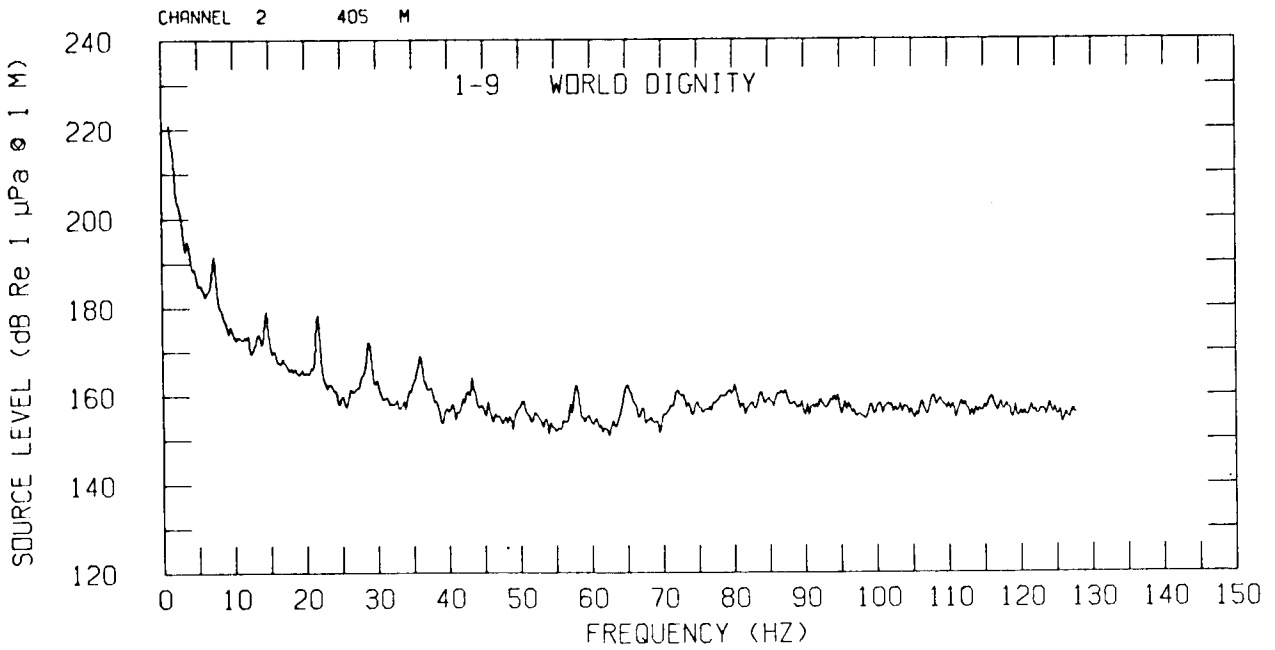
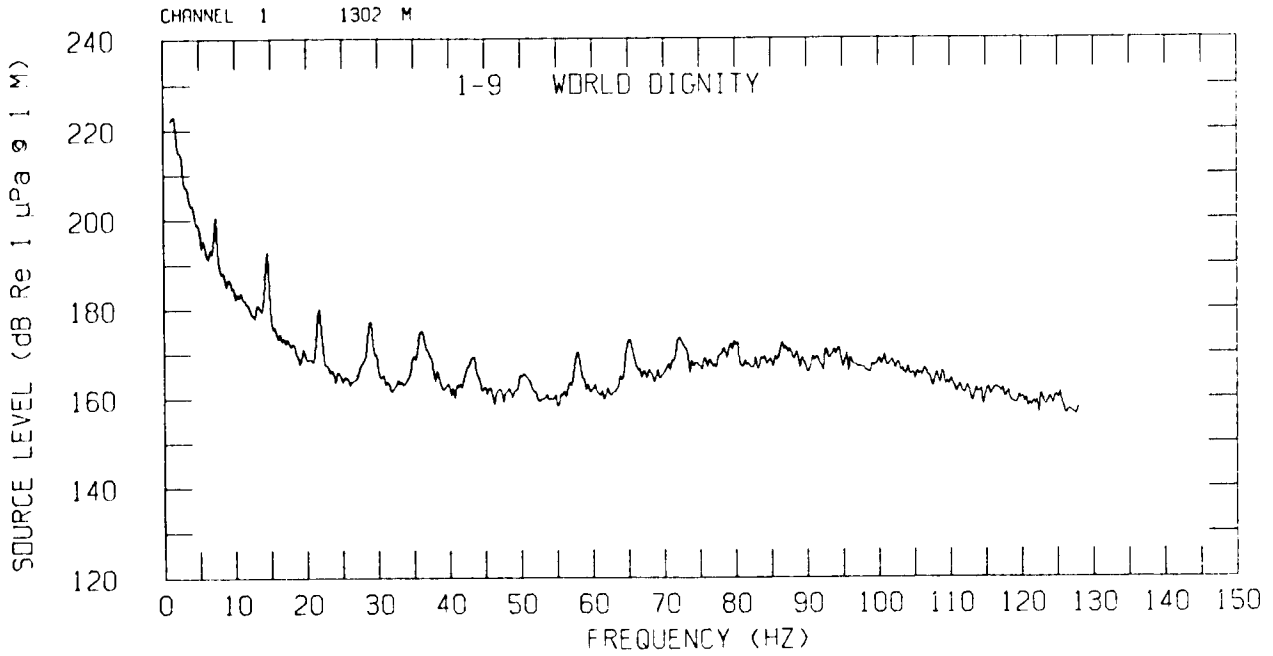
WRIGHT AND CYBULSKI



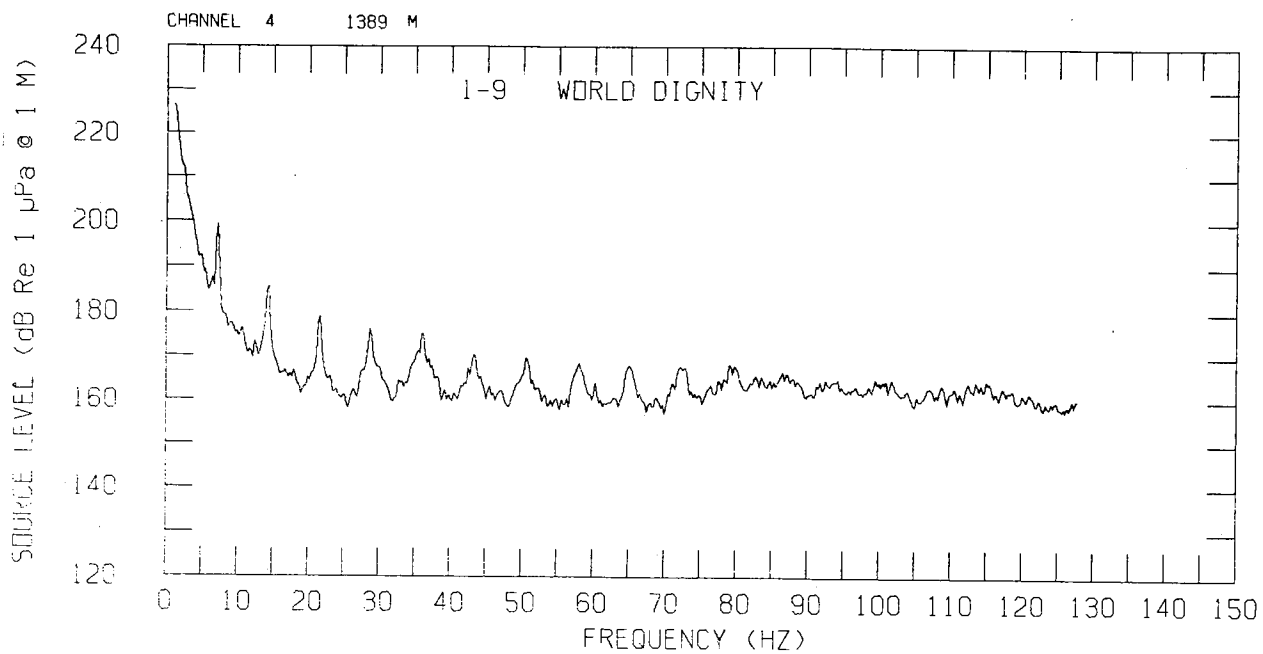
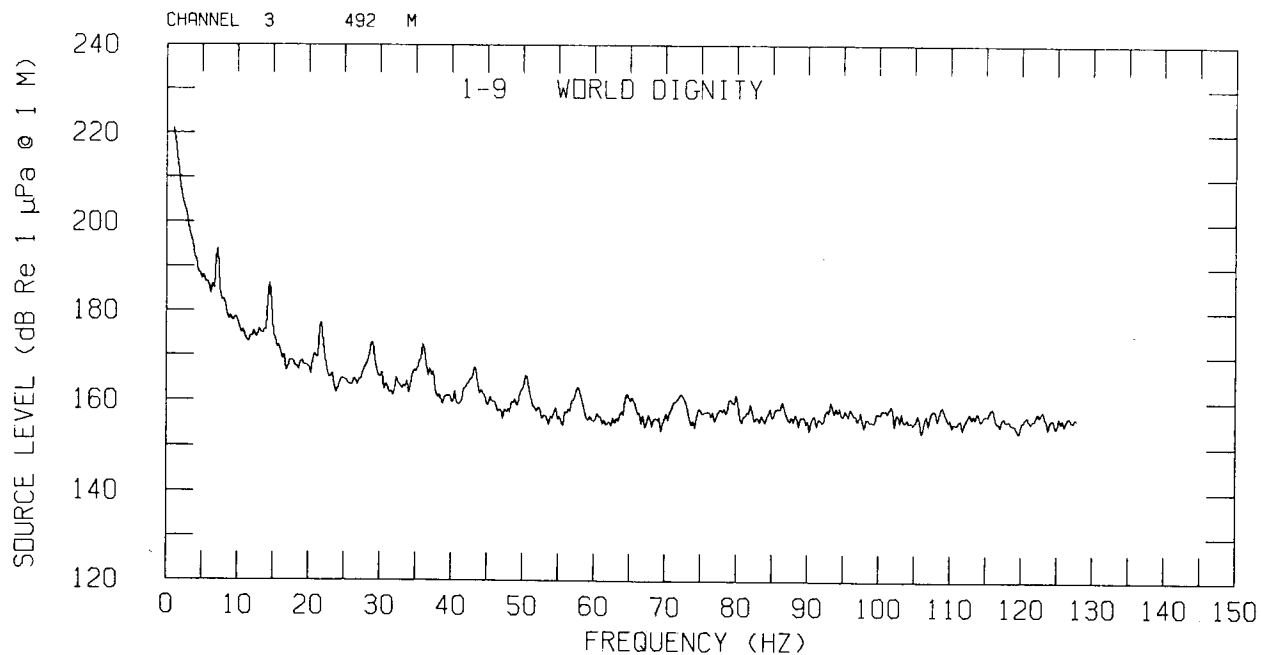


WRIGHT AND CYBULSKI





WRIGHT AND CYBULSKI



Appendix D ERROR ANALYSIS

To assess the relative importance of errors in the various measured and estimated parameters used in computing acoustic source level, we derive some propagation-of-error equations in these parameters. The general technique is:

- Express the computed quantity as a function of the statistically independent variables.
- Compute its total differential as a function of the differential of these independent variables.
- Square this equation and substitute standard errors in the variables for differentials, assuming cross-terms in statistically independent errors vanish in the mean.

First, define a set of symbols for the independent variables and their standard errors:

• Source depth (m)	y_S	S_S
• Receiver depth (m)	y_R	S_R
• Receiver spacing (m)	D	S_D
• Ship speed (m/s)	v	S_v
• Observation time (s)	t	S_t
• Time of CPA (s)	t_0	S_{t_0}
• Received level at hydrophone with calibration error (dB)	RL_k	S_k
• Peak estimate of RL with measurement error (dB)	RL'_k	S'_k

Also define some symbols for derived quantities, with their standard errors:

• Source-receiver slant range (m)	r	S_r
• Range to buoy k at closest approach (m)	x_k	S_{x_k}
• Source level (dB)	SL	S_L

Next, we show the computation of the range at CPA for one of the closest buoys, and compute its standard error, under the general assumption that the ship constitutes an omnidirectional point source, and passes between buoys 1 and 2 with $200 \text{ m} \leq x_1, x_2 \leq 1200 \text{ m}$. For frequencies below 20 Hz, the transmission loss is then on the $40 \log r$ portion of the Lloyd-mirror curve, and we can write approximately

$$RL_k \approx SL - TL_0(y_S, y_R, f) - c \log r_k, \quad \text{where } c \approx 40.$$

Now

$$r_k^2 = x_k^2 + h^2 + v^2(t - t_0)^2, \quad \text{where } h = y_R - y_S.$$

Put $\xi = \eta^2 - 1$, where

$$\eta \equiv \left[\frac{x_2^2 + h^2}{x_1^2 + h^2} \right]^{1/2} = 10^{(RL_1' - RL_2')/c}$$

i.e., η is the slant-range ratio for buoys 1 and 2 at CPA. Then solving for x_1 ,

$$x_1 = \frac{1}{\xi} [\sqrt{(\xi + 1)D^2 - \xi^2 h^2} - D].$$

The standard error for x_1 can then be computed by

$$S_{x_1}^2 = \left[\frac{D^2 - 2\xi h^2}{2\xi(\xi x_1 + D)} - \frac{x_1}{\xi} \right]^2 S_\xi^2 + \left[\frac{(D - x_1)}{\xi x_1 + D} \right]^2 S_D^2 + \frac{\xi^2 h^2}{(\xi x_1 + D)^2} S_S^2 + \frac{(\xi + 1)h^2 + h^2}{(\xi x_1 + D)^2} S_R^2,$$

where, for convenience, the coefficients are in terms of ξ and x_1 , as defined above, and

$$S_\xi^2 = \left(\frac{2 \ln 10}{c} \right)^2 (\xi + 1)^2 (S_1^2 + S_1'^2 + S_2^2 + S_2'^2).$$

Note that the receiver depths of buoys 1 and 2 are treated as statistically independent in the differentiation step.

A general equation for the standard error on source level, as a function of time t and slant range r (or, equivalently, aspect angle), is derived from

$$SL = RL + TL$$

$$dSL = dRL + \frac{\partial TL}{\partial r} dr + \frac{\partial TL}{\partial y_S} dy_S + \frac{\partial TL}{\partial y_R} dy_R,$$

$$\begin{aligned} S_L^2 &= \left\{ 1 + \frac{2x_1}{r^2} \left(\frac{\xi + 1}{\xi} \right) \left[\frac{D^2 - 2\xi h^2}{2(\xi x_1 + D)} - x_1 \right] \right\}^2 S_1^2 \\ &+ \left\{ \frac{2x_1}{r^2} \left(\frac{\xi + 1}{\xi} \right) \left[\frac{D^2 - 2\xi h^2}{2(\xi x_1 + D)} - x_1 \right] \right\}^2 (S_1'^2 + S_2^2 + S_2'^2) \\ &+ \left[\frac{c}{2y_S \ln 10} + \frac{cx_1}{r^2 \ln 10} \cdot \frac{\xi h}{\xi x_1 + D} \right]^2 S_S^2 + \left(\frac{cx_1}{r^2 \ln 10} \right)^2 \left(\frac{D - x_1}{\xi x_1 + D} \right)^2 S_D^2 \\ &+ \left\{ \left[\frac{c}{2y_R \ln 10} - \frac{cx_1}{r^2 \ln 10} \cdot \frac{(\xi + 1)h}{\xi x_1 + D} \right]^2 + \left[\frac{cx_1}{r^2 \ln 10} \cdot \frac{h}{\xi x_1 + D} \right]^2 \right\} S_R^2 \\ &+ \left(\frac{cv}{r^2 \ln 10} \right)^2 (t - t_0)^2 S_v^2 + \left(\frac{cv^2}{r^2 \ln 10} \right)^2 (t - t_0)^2 (S_1^2 + S_0^2), \end{aligned}$$

where we have used

$$\frac{\partial TL}{\partial y_s} \approx \frac{c}{2y_s \ln 10},$$

$$\frac{\partial TL}{\partial y_R} \approx \frac{c}{2y_R \ln 10},$$

$$\frac{\partial TL}{\partial r} \approx \frac{c}{r \ln 10}.$$

As a numerical example, for the ship Lagena at CPA we insert the following values for the observable parameters and estimates of their standard errors:

$$\begin{array}{llll} D = 948 \text{ m} & S_D = 34 \text{ m} & x_1 = 430 \text{ m} & S_r = 0.5 \text{ s} \\ y_S = 12 \text{ m} & S_S = 2.3 \text{ m} & x_2 = 518 \text{ m} & S_0 = 3.1 \text{ s} \\ y_R = 305 \text{ m} & S_R = 3.0 \text{ m} & S_1 = S_2 = 2.1 \text{ dB} & \\ v = 7.5 \text{ m/s} & S_v = 0.1 \text{ m/s} & S_1^1 = S_2^1 = 0.5 \text{ dB} & \end{array}$$

The first few terms of the formula are evaluated as:

$$S_L^2 = 1.01 \text{ dB}^2 + 1.33 \text{ dB}^2 + 2.79 \text{ dB}^2 + \dots$$

so that, under these assumptions, hydrophone calibration error and source depth estimation error each contribute about 1.5 dB to the measurement error. The rest of the terms are negligible.

